This is to certify that the
thesis entitled

BIODEGRADABLE POLYMER NANOCOMPOSITES FROM POLY(ALKYLENE DICARBOXYLATE) AND ORGANICALLY MODIFIED MONTMORILLONITE CLAY

presented by

Ajay Kathuria

has been accepted towards fulfillment
of the requirements for the

MS degree in Packaging

Amar Kumar Mohanty
Major Professor's Signature

12-03-2007
Date

BIODEGRADABLE POLYMER NANOCOMPOSITES FROM POLY(ALKYLENE DICARBOXYLATE) AND ORGANICALLY MODIFIED MONTMORILLONITE CLAY

By

Ajay Kathuria

A THESIS

Submitted to
Michigan State University
in partial fulfillment of the requirements
for the degree of

MASTER OF SCIENCE

Packaging

2007

ABSTRACT

BIODEGRADABLE POLYMER NANOCOMPOSITES FROM POLY(ALKYLENE DICARBOXYLATE) AND ORGANICALLY MODIFIED MONTMORILLONITE CLAY

By

Ajay Kathuria

Packaging is a major consumer of plastics. After use, packaging plastics are discarded, and they end-up as municipal solid waste (MSW). Limited land-fill sites and environmental concerns related to the use of conventional plastics have forced scientists to develop biodegradable materials for packaging applications. Poly(alkylene dicarboxylate) is a class of aliphatic polyester type biodegradable polymers among which poly(butlylene succinate) (PBS) and poly(butylene succinate-co-butylene adipate) (PBSA) are commercially available biodegradable polymers. The reinforcement of these polyesters with organically modified clay can help to improve their mechanical, thermo-mechanical, and barrier properties. The effects of the clay content as well as melt processing cycle time on the mechanical, thermo-mechanical, and barrier properties of the resulting nanocomposites were studied. The storage modulus of PBSA improved by 90 % with 5wt.% organo-clay reinforcement. The thermal behavior of the resulting nanocomposites was studied using Differential Scanning Calorimetry (DSC) and Dynamic Mechanical Analysis (DMA). The morphology of the resulting nanocomposites was evaluated using Transmission Electron Microscopy (TEM) and X-Ray Diffraction (XRD) studies.

ACKNOWLEDGEMENTS

I would like to thank my advisor, Dr. Amar K. Mohanty, for all his support, mentoring, and guidance. His high motivation and new ideas always helped me to gain knowledge and insight into biopolymers. I would like to thank my other committee members: Dr. Bruce Harte and Dr. Farhang Pourboghrat. They were very supportive in the completion of this work and were the source of invaluable advice through our engaging discussions.

The research was made possible through funding received from Center for Food and Pharmaceutical Packaging Research (CFPPR) at School of Packaging, MSU. I am grateful to my colleagues, especially Dr. Mohanty's research group for sharing their knowledge and expertise and helping me in performing my experiments. I would also like to thank the faculty and staff of the School of Packaging, my friends and fellow graduate students who have provided me with a wonderful, friendly atmosphere throughout my Master's program and research period.

Finally, I would also like to thank my parents, my family, my teachers, and my friends for their support, motivation, and help in my day-to-day life.

TABLE OF CONTENTS

LIST OF TABLES

LIST OF FIGURES

Chapter 1

Introduction

Plastics have played a significant role in the development of modern civilization. Plastics have very diverse applications in various fields with substantial contributions in the fields of construction, consumable goods, manufacturing etc. Lightweight plastics used in the automobile, train, and aviation sectors help in reducing energy consumption. Plastics can be divided into two categories: namely, thermosets and thermoplastics. Thermosets are the plastics which cannot be reformed or remolded whereas thermoplastics can be remolded again and again. Thermoplastics and thermosets have their own set of benefits and applications. Thermoplastics have various advantages over thermosets, for example high impact strength, fracture resistance, etc.[1] Thermoplastics have dominated packaging applications because of their desirable tailormade properties. The good chemical resistance of petroleum- based thermoplastics make them an ideal choice for food, chemical, and pharmaceutical packaging.[2] The ease of plastic processing (when compared to metals and glass) and their versatility also played a vital role towards their domination in the packaging industry. Plastics are also known for their light weight, durability, and ease with which they can be easily shaped into various forms. They possess good thermal and electrical insulation characteristics. Plastics processing requires less energy than glass or metals processing and plastics are resilient to corrosion. Market forces such as low cost and convenience also encouraged the use of plastics in

the last couple of decades. Most of the commercially available plastics are conventional petroleum-derived plastics such as polyethylene (PE), polypropylene (PP), polyethylene terephthalate (PET), polystyrene (PS), etc. Conventional petroleum-derived plastics have remarkable properties for a vast range of applications, but they pose serious environmental challenges because of their persistent nature and problems related to disposability. Incineration as an end of the carbon cycle of plastics produces CO_2 and other harmful gases such as carbon monoxide. Recycling of the used plastic goods and plastic waste has not been able to contain the municipal solid waste. Per the 1998 US census, the United States generated 22.4 million tons of plastic waste. Limited petroleum resources and rising crude petroleum prices are also affecting the economics of the plastic and packaging industry. Agricultural raw materials like corn and sugarcane, if utilized for the production of the monomers, can provide impetus to the rural economy by generating additional rural employment. Bio-based material can be helpful in catapulting the economy in the next orbit of economic growth. In today's fast-changing global political landscape, bio-based materials are strategically important to reduce the dependency of various nations on petroleum-based resources which are concentrated in certain geographies of the world. The scientific and industrial communities around the world are working in tandem for the development of alternative eco-friendly, biodegradable, and sustainable packaging materials. [3, 4]

Biodegradable plastics are the polymers that can decompose with the aid of microbial or enzymatic action when subjected to suitable composting conditions. Biodegradable polymers present a challenging opportunity. A lot of scientific research is focused on the development [5-10] and commercialization of biodegradable polymers. They can be obtained from renewable resources like corn, starch, wood cellulose, etc. However, they can also be derived from the petrochemicals resources. Due to comparatively higher cost, small-scale, and certain properties limitations biodegradable polymers in general are not prevalent in the mainstream of plastic industry. Although biodegradable polymers have started making inroads into the commercial applications, there is lot of potential in the improvement of their properties for large scale or mass level applications. Some of the widely available biodegradable polymers are polylactic acid (PLA), polyhydroxybutyrate (PHB), poly (alkylene dicarboxylate), poly (butylene adipate terephthalate) (PBAT), poly (ε-caprolactone), thermoplastic starch, etc.

Poly(alkylene dicarboxylate) is a class of biodegradable aliphatic polyester prepared by polycondensation reaction of glycols and dicarboxylic acids.[11] Poly(alkylene dicarboxylate)s are commercially prepared by Showa High Polymers Co. Ltd., Japan under the trademark "Bionolle." These polymers are quite similar to the polyolefin family of polymers, but they possess poor melt viscosity. Poly(alkylene dicarboxylate) polymers have relatively poor water and gas barriers as compared to polyolefins. Bionolle has excellent processability. It can be processed into melt blow, multifilament, monofilament, nonwoven, flat,

and split yarn in the field of textiles and also into injection-molded plastics products, thus being a promising polymer for various potential applications including packaging. Bionolle can be processed on polyolefin machines at temperatures of 100-230°C. Some examples of its potential applications include shampoo bottles, beverage bottles, food trays, shopping bags, cups, drug bottles, etc. Bionolle can take between 2 to 6 months to degrade under composting conditions. Bionolle has a promising future since succinic acid used for the production of some of the polymers of this class can be derived from biobased materials.[11] Various chemical companies are in the process of developing the technology to produce succinic acid from biobased resources at bulk level. Therefore, the poly(alkylene dicarboxylate) class of polymers can be categorized into the green and sustainable class of polymeric materials.

Polymer composites are prepared by a combination of two or more materials such as reinforcement, matrix, fillers which differ in the form on macro-scale. The constituents retain their identities. They do not dissolve or merge into each other, although they act in concert. Normally, the components can be physically identified and exhibit an interface between each other. Some of the common reinforcements are glass fibers, silica, minerals, and natural fibers. A lot of research has been done on glass fiber composites [12-17]. Glass fibers have been commercially used in the automobile industry and for structural applications. Natural fibers such a kenaf, jute, flax, hemp, and sisal have attracted a lot of attention [18] because they are widely available, and they are

renewable in nature. Natural fibers have advantages over glass fibers such as low cost, low density, ease of separation, and abundant presence. Natural fibers are biodegradable in nature. Fabrication of polymer composites using natural fibers such as flax, hemp, or jute is a good technique to improve the physical, mechanical, and thermo-mechanical properties of polymers [19-23]. The improvement in the properties of composites depends upon the amount of stress transfer from the polymer matrix to the filler [24]. The size of filler, amount of the filler [25], compatibility of the filler with the polymer matrix, distribution of the filler [26], and its intimate contact with the polymer matrix play an important role in the stress transfer. Conventional fibers or fillers also help to reduce the cost of the end product. As compared to conventional fillers, a small amount of nano fillers such as nano talc, layered silicates show a lot of improvement due to their high aspect ratio and nano level interactions.

Nano means one billionth, and nanotechnology refers to one billionth of a meter. As defined by The Royal Society, London "Nanotechnologies are design, characterization, production and applications of structures, devices and systems by controlling shape and size at nanometer scale." [27] The materials having atleast one dimension in the range of 1 to 100 nanometers are categorized as nano materials. Nano material can be classified into three categories: (i) nano materials having all three dimensions in the nano range (for example, spherical silica); (ii) nano materials having all two dimensions in the nano range (for example, carbon nano tube); and (iii) nano materials having one dimensions in

the nano range (for example layered silicate). Carbon nano tubes, organically modified layered silicates, nano-talc, and cellulose whiskers are popular nano materials. Layered silicates are popular for the production of polymer nanocomposites because they improve the barrier properties of polymer which is crucial for food and pharmaceutical packaging applications. The interactions between layered silicates and polymer matrix have attracted a lot of attention in the scientific community [28-32]. The nano-reinforcement of the polymer matrix with organically modified layered silicates is an exciting area to improve the mechanical and thermo mechanical properties of the polymer. Organically modified layered silicates (organo-clay) can reduce the flame retardancy [33-37] and increase the heat deflection temperature (HDT) of the nanocomposites as compared to virgin polymers [38-41]. Montmorillonite, hectorite, and saponite organo-clays belong to the smectite group of the clay minerals. These clays are popular because of good intercalation capabilities. Montmorillonite clay has been extensively used for various polymer-nanocomposite studies. The main constituent of montmorillonite is organic ash called bentonite. Each platelet of montmorillonite clay consists of Al octahedral sheet sandwiched between two Si tetrahedral sheets. Isomorphic substitution in the sheets creates deficit of positive charge which is balanced by the Na^+ charge present in the interlayer or d-spacing region. Clay in its natural state is hydrophilic in nature because of the presence of hydroxyl groups in the structure while the majority of the polymer matrix are hydrophobic in nature because of the presence of long hydro-carbon chains. Therefore clay in its natural state is not compatible with the polymers. To

make clay compatible with the polymer matrix organically modified clays have been investigated [42-47]. The organic modification involves the replacement or substitution of Na^+ ions present in gallery or d-spacing. Organic modification reduces the surface energy of the clay and increases the interlayer spacing (d-spacing) between the clay platelets [48]. Organic modification of the clay also increases the interfacial interaction between the polymer matrix and the clay platelets [49]. These organically modified clays are also called nanoclay because of the separation of the clay platelets. Each clay platelet being 1 nanometer thick can be classified into the nano-material category.

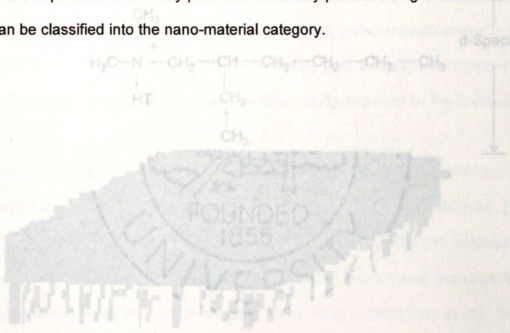

Fig 1.1: Organically Modified Clay

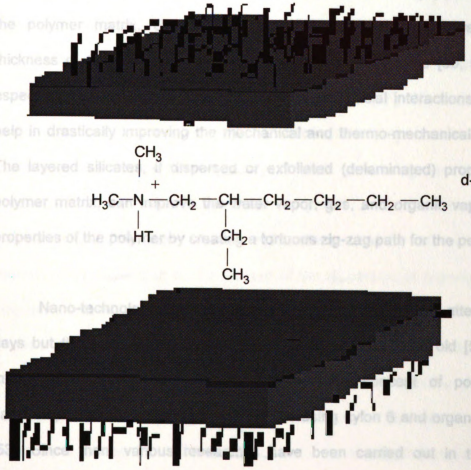

Fig 1.1: *Organically Modified Clay*

Organically modified layered silicates are prepared by replacing the Na^+ or K^+ ions in the silicate layer with quaternary alkylammonium or alkylphosphonium cations. These cation exchange reactions increase the organophilicity of the clay thus helping in improving the interfacial interactions of the layered silicates with the polymer matrix. Organically modified layered silicates have a typical thickness of 1 nanometer and an aspect ratio of 10 to 1000 [50, 51]. A high aspect ratio of layered silicates increases the interfacial interactions which can help in drastically improving the mechanical and thermo-mechanical properties. The layered silicates, if dispersed or exfoliated (delaminated) properly in the polymer matrix, can improve the water vapor, gas, and organic vapors barrier properties of the polymer by creating a tortuous zig-zag path for the permeants.

Nano-technology and nanocomposites are getting a lot of attention these days but the science of nanocomposites is around 50 years old [52]. Toyota motor company was the first to introduce the concept of polymer clay nanocomposites for automotive applications using nylon 6 and organophilic clay [53]. Since then, various researches have been carried out in the field of polymer-layered silicate nanocomposites. The reinforcement of polymer with the nanoclay can improve mechanical, thermomechanical, and barrier properties as well as flame retardancy [54, 55]. Some researchers have also evaluated the effect of nano-reinforcement on the biodegradation of the biodegradable polymers. Kazauki et. al. [56] established that the preparation of nanocomposites

can help in increasing the biodegradability of nanocomposites in composting conditions.

Nanocomposites can be prepared by three different techniques: in situ polymerization, solvent casting, and melt processing of the polymer with the organo-clay [Fig. 1.2]. In situ polymerization and solvent casting techniques have limited utilization because of the unavailability of suitable monomer or compatible solvent solution for all the nanocomposites systems [57]. The melt processing technique is more popular for the preparation of the polymer nanocomposites. Important reasons for the popularity of melt processing are: low cost of production and high volume capacity as compared to solvent casting and in situ polymerization. We can obtain three different kinds of nanocomposite morphologies depending on the degree of the dispersion of organo-clay in the polymer matrix: agglomerated, intercalated, exfoliated, and flocculated nanocomposites. Schematic representation of the polymer-clay nanocomposites is shown in Fig. 1.3 [58]. Some of the factors which affect the polymer clay nanocomposites are the processing conditions of the polymer-nanoclay, interactions between nanoclay and the polymer matrix, clay loading, etc.

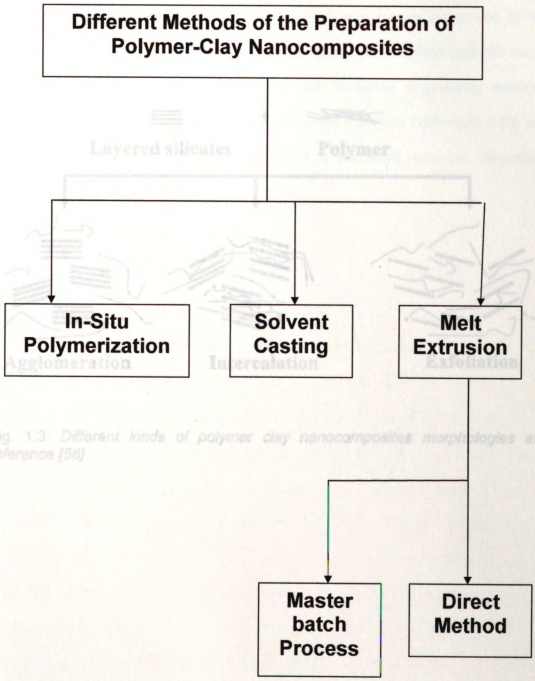

Fig 1.2: *Schematic representation of different methods of nanocomposites preparation*

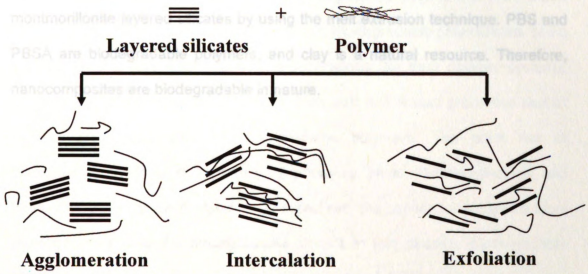

Fig. 1.3: *Different kinds of polymer clay nanocomposites morphologies after reference [58]*

The aim of this study was to prepare biodegradable nanocomposites and to improve the mechanical, thermo-mechanical, and barrier properties of the biodegradable polymers. We investigated polymer clay nanocomposites using PBS and PBSA matrices with commercially available organically modified montmorillonite layered silicates by using the melt extrusion technique. PBS and PBSA are biodegradable polymers, and clay is a natural resource. Therefore, nanocomposites are biodegradable in nature.

Chapter 2

Background and Literature Review

The production and application of biodegradable polymers in the medical field can be traced back to the 1970's [59, 60]. Biodegradable polymers are being used in various high value biomedical applications like drug delivery systems, sutures, and orthopedic parts. However, high cost and limited properties restrict the ecological application of biodegradable polymers. The price rise of conventional plastic resin, technological advances, environmental concerns, and public awareness of the problems associated with the conventional plastics have provided impetus to the biodegradable plastics in last decade. Biodegradable plastics are now acquiring center stage in the development of polymer science and technology. The industrial community has developed different technologies to prepare biodegradable polymers from renewable resources, petroleum-based resources, or a combination of both renewable and non-renewable resources. Degradation of the polymers is independent of its origin. It is the intrinsic property of the chemical structure of the repeating unit in the polymeric structure. Standard authorities around the world have set up different standards tests for biodegradable polymers. The International Standard Organization (ISO-472-1988) has characterized biodegradable plastics as plastics which go through chemical changes under particular environment. These polymers experience change in their properties. The changes in the property of biodegradable plastics are a results of natural process prompted by microorganisms [61]. The American

Society of Testing Material (ASTM Subcommittee D20-96) has classified biodegradable plastic as plastic in which the degradation of chemical structure takes place as a result of micro-organisms such as bacteria, fungi and algae [62].

On the basis of origin we can divide biodegradable polymers into three classes: renewable resource-based biodegradable polymers, petroleum-based biodegradable polymers, and Petro-Bio mixed. Biopolymers can be derived from renewable resources like corn, cellulose, and sugar. Bionolle™ is a class of aliphatic polyesters. It is available in a variety of grades such as poly(butylene succinate)(PBS), poly(butylene succinate-co-adipate) (PBSA), poly(ethylene succinate), poly(ethylene succinate-co-adipate). PBS and PBSA are commercially available biodegradable polymers in this class of aliphatic polyesters. Chemical Structure of Poly(alkylene dicarboxylate) is represented in Figure 2.1.

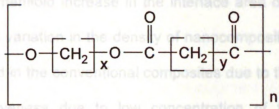

Fig 2.1 *Structure of poly(alkylene dicarboxylate)*
PBS Where, X=4 and Y=2
PBSA Where, X=4 and Y=2 or 4

Figure 2.2 [62, 63] shows the classification of biodegradable polymers on the basis of their origin. Fujimaki reported that food trays, cups, vessels, shampoo bottles, cosmetic bottles, composting bags, shopping bags, shrink film, etc. are some of the potential applications of Bionolle.™ [64] However barrier properties, softness, and thermal stability obstructed its mass-level applications. The improvement in the performance and properties of PBS and PBSA can help in expediting the transition from conventional polymers to biodegradable polymers. Different techniques can be employed to improve the properties of the polymers such as blending, composite fabrication, etc. Composite fabrications are popular techniques followed by engineers and scientists for the improvement in the performance and properties of the polymers. Glass fiber reinforced composites and wood fiber composites have traditionally been utilized by various industries. However, nano-materials are gaining a lot of attention these days. The layered silicate nanocomposites contain small amount of modified layered silicates (1-5 weight %) where as conventional composites have high percentage of the filler in the polymer matrix, generally in the 20-40%. High aspect ratio of the layered

silicates leads to manifold increase in the interface area of the filler and matrix. There is not much variation in the density of nanocomposites with respect to the matrix as observed in the conventional composites due to the bulk addition of the filler. Cost effectiveness due to low concentration of filler can be another favorable reason to select nanocomposites over conventional composites.

Figure 2.2 *Classification of Biopolymers [62, 63]*

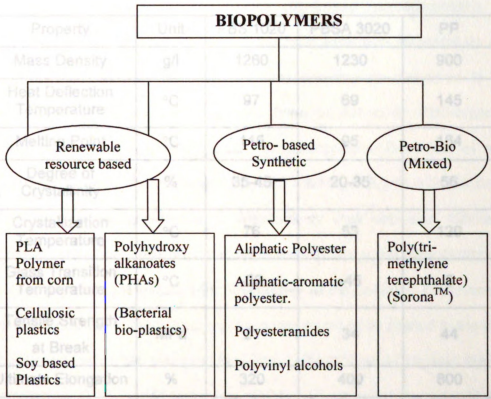

Table-2.1 Material Properties of PBS and PBSA [73]

Property	Unit	PBS 1020	PBSA 3020	PP
Mass Density	g/l	1260	1230	900
Heat Deflection Temperature	°C	97	69	145
Melting Point	°C	115	95	164
Degree of Crystallinity	%	35-45	20-35	56
Crystallization Temperature	°C	76	53	120
Glass Transition Temperature	°C	-32	-45	5
Tensile Strength at Break	MPa	21	34	44
Ultimate Elongation	%	320	400	800
Flexural Modulus	MPa	580	340	1370
Structure	-	Linear	Linear	Linear

The addition of organically modified layered silicates in the polymer matrix is an innovative novel technique to improve the mechanical, thermo-mechanical, and barrier properties of the polymers. Nanocomposites are also known for better heat deflection temperature as compared to virgin polymers. E. Manias et al [65] studied the polypropylene-montmorillonite clay-based nanocomposites. They observed around 40% improvement in the heat deflection temperature of PP nanocomposites with the addition of 6% organo-clay as compared to virgin polymer. Various research studies have been published on PBS-organoclay nanocomposites and PBSA-organoclay nanocomposites. Bousmina et al [66] have studied Cloisite 15A, Cloisite 93 A, and Cloisite 30B with a PBSA polymer matrix. The nanocomposites were prepared by melt extrusion followed by compression molding. They observed improvement in the mechanical properties. The nanoclay particles reduced the crystallinity of the polymer. Improvement in the thermal stability of the nanocomposites was found to be related to the degree of the dispersion of the nanoparticles. Five different kind of organic modifiers: dodecylamine (DA), octadecylamine (ODA), 12-aminolauric acid (ALA), N-lauryldiethanolamine (LEA) and 1-[N,N-bis(2-hydroxy-ethyl)amino]-2-propanol (HEA) were utilized by Someya et al [67] to study the effect of modification on the properties of PBS and organically modified clay based nanocomposites. They have reported that the higher degree of intercalation showed higher tensile modulii and lower tensile strength. An increase in the tensile modulus can be related to better dispersion. The decrease in tensile strength was attributed to the

decrease in elongation at break. The nanoparticles increased the glass transition temperature and promoted the crystallinity by acting as nucleating agents.

Chen et. al. [68, 69] have studied PBS and PBSA with Cloisite 25A and twice functionalized organoclay nanocomposites. Twice functionalized clay (TFC) was prepared by the reaction of glycidoxypropyl trimethoxy silane (GPS) with the silanol groups on Cloisite 25A. These studies evaluated the mechanical properties, morphology, and viscoelastic properties. The improvement in mechanical properties was observed up to 5 wt.% of Cloisite 25A and TFC. They observed better dispersion of the twice functionalized clay (TFC) than the Cloisite 25A which indicated better interactions between TFC and the polymer matrix. Okamato et. al. [56] studied PBS with montmorillonite clay modified with octadecylammonium cation, octadecyl trimethyl ammonium cation, and saponite clay modified hexadecyltributylphosphonium cation. They studied the mechanical, thermomechanical, oxygen barrier properties and biodegradability of the nanocomposites film. The biodegradability of nanocomposites was conducted under soil field and in the composting conditions. After 35 days, it was observed that the nanocomposites film degraded faster than the neat film in the composting condition. The films' surface showed signs of degradability after 6 months under soil field conditions. The rate of degradation of the films was independent of the type of montmorillonite clay modification. In the case of modified saponite clay, the degradation rate was high, which may be because of the presence of an alkylphosphonium surfactant. Oxygen gas permeability

decreased for all the PBS-organoclay compositions. The oxygen barrier properties improved by approx. 45% for PBS and 3.6% octadecylammonium modified montmorillonite clay.

Ray et. al. [70] also published a study on PBS-C_{18}–mmt nanocomposites. They observed remarkable improvement in the mechanical properties. The morphological studies revealed that the clay platelets were intercalated and randomly distributed in the polymer matrix. Research has been conducted on PBS/glass fiber composites [71] prepared by electron beam irradiation in the presence of cross linking agent. The polymer matrix was found to be degradable, and the glass fiber needed to be collected from the composting facilities for recycling purposes.

Jo Ann Ratto et. al. [72] studied blends of PBSA and starch composites. The starch composition was varied from 5 to 30% in the PBSA matrix. The mechanical and thermo-mechanical properties along with the biodegradability of the extrusion blown PBSA/ starch film were evaluated. The tensile strength and toughness of the film decreased with the increase in the starch content in the PBSA matrix. Biodegradability of the PBSA films increased with the addition of the starch in the PBSA matrix. The biodegradability of the composites was supported by the respirometric test and scanning electron microscopic studies.

The objective of this research was to prepare biodegradable PBS and PBSA-organo-clay nanocomposites with improved mechanical, thermomechanical, and barrier properties for packaging applications. Organically modified montmorillonite clay based nanocomposites were fabricated by melt extrusion followed by the injection molding process. The effect of temperature, clay content, and cycle time of compounding on the mechanical properties and thermo-mechanical properties of the resulting nanocomposites were studied. The oxygen and water vapor permeability of the compression-molded nanocomposites films were evaluated and compared with other conventional polymers. The resulting nanocomposites properties were verified through Transmission Electron Microscopy (TEM) and X- ray Diffraction (XRD) studies.

Chapter 3

Materials and Methods

3.1 Materials

3.1.1 Poly(butylene succinate):

Poly(butylene succinate) ("Bionolle 1020") was supplied by Showa High Polymers Co. Ltd., Japan under the tradename "Bionolle". It is prepared by condensation polymerization of 1, 4 butanediol with succinic acid. "Bionolle 1020" is an injection grade polymer having density of 1.25 g/cc and its melting point is 115°C [64,73]. PBS 1020 is biodegradable under composting conditions. The plastic pellets were dried in the vacuum oven at 70°C for 24 hrs before processing. The structure of PBS is shown in Fig. 3.1. PBS has a promising future because both the monomers used in the condensation polymerization of PBS (i.e., succinic acid and 1, 4 butanediol) can be obtained from the renewable resources such as corn, sugarcane, etc. Table 3.1 represents various properties of PBS 1020 and PBSA 3020.

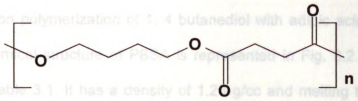

Fig 3.1 *Structure of Poly(butylene succinate)*

Table 3.1. Properties of PBS 1020 and PBSA 3020 [64, 73]

Property	PBS 1020	PBSA 3020
Melting Point (°C)	114-115	93-95
Density (g/cc)	1.26	1.23
Tensile Elongation (%)	320	400
Tensile Strength at Break (MPa)	21	34
Crystallization Temperature (°C)	76	53
Glass Transition Temperature (°C)	-32	-45

3.1.2 Poly(butylene succinate-co-adipate) (PBSA)

Poly(butylene succinate-co-adipate) ("Bionolle™ 3020") is an injection grade copolymer supplied by Showa High Polymer Co. Ltd, Japan. It is prepared by condensation polymerization of 1, 4 butanediol with adipic acid and succinic acid. The Chemical structure of PBSA is represented in Fig. 3.2. Its properties are listed in Table 3.1. It has a density of 1.23 g/cc and melting temperature of 95°C. [64, 73] The pellets were dried at 65°C for 24 hrs before processing.

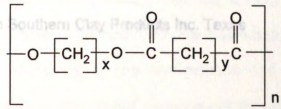

Figure 3.2. *Structure of Poly(butylene succinate-co-adipate) Where, X=4 and Y=2 or 4*

3.1.3 Organically Modified Montmorillonite Clay. The organically modified montmorillonite, Cloisite 25A™, is a commercial product of Southern Clay Products Inc., Texas. This clay is modified with dimetyl, hydrogenated tallow, 2-ethylhexyl quaternary ammonium cation. The structure of the organic modifier is shown in Figure 3.3.

Table 3.2. Characteristics of Organically Modified Montmorillonite Clay

OMMT Clay	XRD Basal Spacing d_{001}(nm)	Extent of Modification [meq/100g clay]	Specific Gravity (g/cc)
Cloisite 25 A*	**1.86**	**95**	**1.87**

*Data obtained from Southern Clay Products Inc. Texas

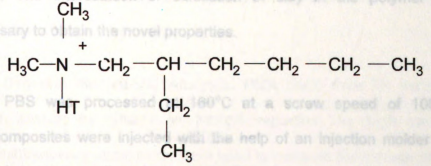

Fig. 3.3: *Structure of the organic modifier used for cation exchange reaction of Cloisite 25A*

3.2 Methods. There are two methods of nanocomposite preparation: direct blending and masterbatch-based blending. The masterbatch melt blending technique was used in this study to prepare PBS-Cloisite 25A and PBSA-Cloisite 25A nanocomposites. The DSM micro-compounding instrument was used to fabricate the masterbatch and the desired nanocomposite compositions. There were two steps used for the preparation of nanocomposites. In the first step, the masterbatch of PBS or PBSA and Cloisite 25A was prepared using high weight% of clay concentration. The masterbatch was extruded as strands and then palletized in the pelletizer. In the second step, the desired compositions of the polymer and organoclay were prepared from the masterbatch and neat polymer. The main reason for using a two-step process for the preparation of nanocomposites was to achieve better dispersion of organoclay in the polymer matrix. The intercalation or exfoliation of clay in the polymer matrix was necessary to obtain the novel properties.

PBS was processed at 160^{o}C at a screw speed of 100 rpm. The nanocomposites were injected with the help of an injection molder attached to the micro-compounding instrument. The injection mold temperature was maintained at 45^{o}C. Injection pressure was set at 100 psi. The PBS-3% 25A and PBS-5% 25A nanocomposites were prepared at 5 mins., 10 mins. and 15 mins. of melt processing cycle time to evaluate the effect of processing conditions on the performance of the resulting nanocomposites.

PBSA was processed at two processing temperatures: 125°C and 140°C. The melt extrusion was followed by the injection molding technique. The mold temperature was maintained at 40°C with injection pressure of 100 psi. The process cycle time was varied from 5 mins. to 20 mins. at a screw speed of 100 rpm.

3.3 Equipments and Preparation

3.3.1 DSM Microcompounder. The DSM micro-compounding instrument consists of two vertical screws having a length of 150 mm. The volume of micro-compounding instrument is 15cc, and it has an L/D ratio of 18. The micro-compounder is attached to an injection molding unit. The injection molding unit has different designed standard molds to prepare samples for tensile testing, DMA testing, XRD samples, etc.

3.3.2 Dynamic Mechanical Analysis. DMA Q800 from TA Instruments was used to analyze the dynamic mechanical properties. The single cantilever mode and multifrequency strain mode were used to measure the storage modulus, loss modulus, and tan delta over the temperature range of -80°C to 70°C at a frequency of 1 hz and an amplitude of 15 μm.

3.3.3 Tensile Properties. The dog-bone tensile samples were prepared by injection molding. The tensile properties such as % elongation at break and tensile strength were measured using the Universal Testing Machine (UTS,

Model SFM-20) as per ASTM D-638 using a gauge length of 1 inch. A load cell of 1,000 lbs was utilized for the testing at a crosshead speed of 20 in./min. At least five specimens were used for all property evaluations.

3.3.4 Film Preparation. Nanocomposite films were prepared by compression molding technique with the help of a compression molding machine of an area 9" x 9". The PBSA and PBS nanocomposites disc samples were compressed at 120°C and 150°C, respectively, using a force of 6,000 pounds for 2 minutes. The compression-molded films were used for evaluating the permeability characteristics of the PBS and PBSA nanocomposites.

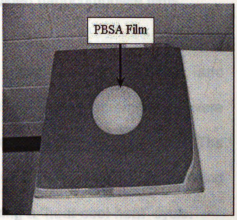

Fig 3.4: *PBSA Film prepared by compression molding*

3.3.5 Measurement of Water Permeability. The water vapor transmission rate was measured by using MOCON PERMATRAN-W 3/33 (MOCON Inc., US). The permeability values of PBS and PBSA nanocomposites films were calculated from the Water Vapor Transmission Rate (WVTR) data. The tests were carried out at a temperature of 37.8°C and 100% relative humidity. In analyzing the data, three specimens of each sample were exposed by using aluminum masks of 1cm^2 area.

3.3.6 Measurement of O_2 Gas Permeability. The O_2 gas transmission rate of PBS and PBSA nanocomposites films were measured with the help of MOCON OXTRAN-2/21 (MOCON Inc., US). The tests were performed using 100% O_2 gas concentration at a temperature of 23°C. The aluminum masks were used to expose an area of 1 cm^2 area of compression-molded nanocomposite films.

3.3.7 Differential Scanning Calorimetry.The glass transition, melting, and crystallization temperatures of the PBS and PBSA nanocomposites were measured using a Q100 (TA instruments) differential scanning calorimeter. The tests were carried out at the temperature range of -80°C to 140°C at a scanning rate of 10°C/min. The materials were scanned using a "heat-cool-heat" cycle.

3.3.8 Izod Impact Tester. A Monitor Izod Impact tester (Testing Machines Inc., USA, Model TMI® 43-02-01) was used with a 5-pound pendulum to notched Izod Impact strength of samples at ambient conditions according to the ASTM D256 standard. A TMI notching cutter (Model-22-05) was used to notch the samples as per the standard. The notched samples were conditioned for at least 48 hours at 23°C and 50% RH before testing. At least five specimens were used for each sample in evaluating the notched Izod impact test.

3.3.9 X-Ray Diffraction. The XRD characterization of nanocomposites was used to study the morphological characteristics of the resulting nanocomposites. The Bragg's equation $n\lambda = 2 d \sin\theta$ [where; λ is the wave length of the light, d is the

distance between the clay platelets, θ is the angle of incidence] was used to calculate interlayer spacing between clay platelets of the organo-clay and the clay platelets dispersed in the polymer matrix. Experiments were performed at a wavelength of 0.01541838 nm.

3.3.10 Transmission Electron Microscopy (TEM). The morphological behaviors of the nanoclay platelets in the PBS and PBSA nanocomposites were observed using Transmission Electron Microscopy (TEM). Cryogenically microtomed ultra thin film specimens of the nanocomposites with a thickness of approximately 70 nm were used for the TEM observations. The microtoming was carried out at –130°C using the ultramicrotomy with a cryogenic attachment and diamond knife. A Joel 100 CX TEM with LaB6 filament in 100kV accelerating voltage was used for observing the TEM images of nanocomposites.

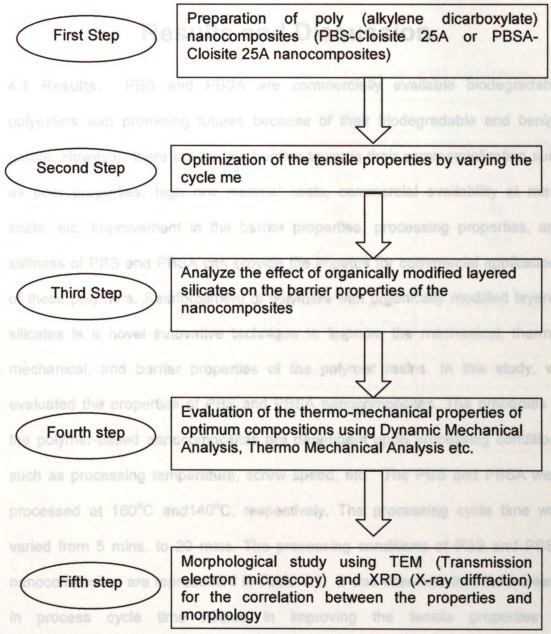

Figure 3.5: *Schematic representation of steps followed for this research work*

Chapter 4

Results and Discussion

4.1 Results. PBS and PBSA are commercially available biodegradable polyesters with promising futures because of their biodegradable and benign nature. However, there are certain hurdles towards their commercialization such as poor properties, high raw material costs, commercial availability at mass scale, etc. Improvement in the barrier properties, processing properties, and stiffness of PBS and PBSA can provide the impetus for commercial applications of these polymers. Reinforcement of polymers with organically modified layered silicates is a novel innovative technique to improve the mechanical, thermo-mechanical, and barrier properties of the polymer resins. In this study, we evaluated the properties of PBS and PBSA nanocomposites. The properties of the polymer-based nanocomposites are dependent upon processing conditions such as processing temperature, screw speed, etc. The PBS and PBSA were processed at 160°C and140°C, respectively. The processing cycle time was varied from 5 mins. to 20 mins. The processing conditions of PBS and PBSA nanocomposites are represented in Table 4.1. It was observed that the increase in process cycle time helped in improving the tensile properties of nanocomposites.

Table 4.1. *Processing Conditions Used in Nanocomposites Fabrication*

Processing Conditions			
Parameter	Unit	PBS-Cloisite 25A	PBSA-Cloisite 25A
Processing Temperature	°C	160	140
Injection Mold Temperature	°C	45	40
Screw Speed of Extruder	Rpm	100	100
Injection Pressure	Psi	100	100
Processing Time	Min	3 to 15 Minutes	3 to 20 Minutes
Drying Temp. (Polymer)	°C	65	65
Drying Time (Polymer)	-	Overnight	Overnight
Drying Temp. (Clay)	°C	80	80
Drying Time (Clay)	Hour	6	6

Part I

PBSA 3020 - Cloisite 25A

Nanocomposites

4.1.1 Tensile Properties of PBSA-Cloisite 25A. The Elongation of PBSA-3% Cloisite 25A and PBSA-5% Cloisite 25A are represented in Figures 4.1 and 4.2, respectively. Some important factors that can affect the tensile properties of the polymer clay nanocomposites are aspect ratio of the clay, polymer-organoclay compatability, dispersion of clay in the polymer matrix, etc. The processing conditions such as processing cycle time or residence time and screw speed are also important as they can affect the dispersion of the clay platelets in the polymeric matrix.

The optimum properties for PBSA-3% 25A and PBSA-5% 25A were observed at 15 mins and 20 mins processing cycle time, respectively, under the present experimental conditions. One of the general observations from these tensile tests was the improvement of the consistency in the properties of the PBSA-Cloisite25A nanocomposites with the increase in the cycle time that is supported by lower values of standard deviation at a higher cycle. It was observed that an increase in cycle time helped in improving % elongation at break. This could be explained by the better dispersion of the organo-clay in the polymer matrix which lead to better energy dissipation mechanism. At the lower processing cycle time, the elongation values dropped drastically. This might be attributed to the possible agglomeration of the clay. This was due to the fact that the cracks were usually initiated and propagated through the agglomerates to provoke the failure of the samples [74]. The d-spacing between the clay platelets of Cloisite 25A was 1.8 nm [75]. The XRD of PBSA-3% 25A at 15 mins. processing cycle time indicated exfoliation of the clay platelets whereas in the

case of PBSA-5% 25A, the d spacing increased to 3.2 nm. The increase in the interlayer spacing of the clay platelets in the polymer matrix supports intercalation of the polymer matrix in the clay platelets. These results were further elucidated with the help of the TEM studies.

Figure 4.1: Comparison of percentage elongation of PBSA and PBSA -3% Cloisite 25A nanocomposites

A = PBSA (3 min processing time)
B = PBSA-3% Cloisite 25A (10 min processing time)
C = PBSA-3% Cloisite 25A (15 min processing time)
D = PBSA-3% Cloisite 25A (20 min processing time)

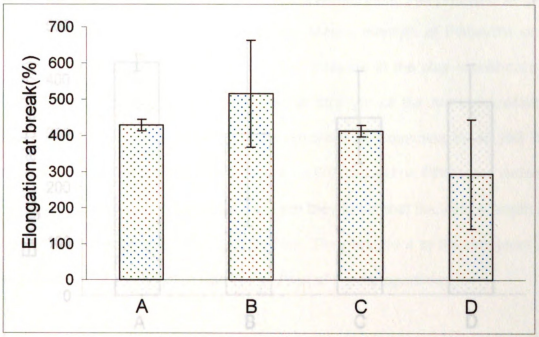

Figure 4.1: *Comparison of percentage elongation of PBSA and PBSA -3% Cloisite 25A nanocomposites*

A = PBSA (3 min processing time)
B = PBSA-3% Cloisite 25A (10 min processing time)
C = PBSA-3% Cloisite 25A (15 min processing time)
D = PBSA-3% Cloisite 25A (20 min processing time)

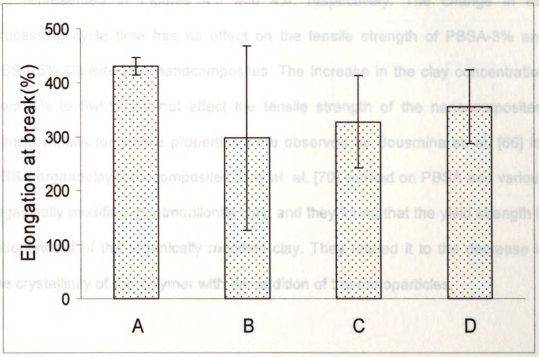

Figure 4.2: *Comparison of percentage elongation of PBSA and PBSA -5% Cloisite 25A nanocomposites*

A = PBSA (3 min processing time)
B = PBSA-5% Cloisite 25A (10 min processing time)
C = PBSA-5% Cloisite 25A (15 min processing time)
D = PBSA-5% Cloisite 25A (20 min processing time)

The tensile strength of PBSA-3% 25A and PBSA-5% 25A at varying cycle times are represented in Figures 4.3 and 4.4, respectively. The change in the processing cycle time has no effect on the tensile strength of PBSA-3% and PBSA-5% Cloisite 25A nanocomposites. The increase in the clay concentration from 3% to 5wt.% did not affect the tensile strength of the nanocomposites. Similar results for tensile properties were observed by Bousmina et. al. [66] for PBSA-organoclay nanocomposites. Ray et. al. [70] worked on PBSA and various organically modified montmorillonite clay, and they found that the yield strength is independent of the organically modified clay. They related it to the decrease in the crystallinity of the polymer with the addition of the nanoparticles.

Figure 4.3: Comparison of tensile strength of PBSA and PBSA-3% Cloisite 25A nanocomposites

A = PBSA (3 min processing time)
B = PBSA-3% Cloisite 25A (10 min processing time)
C = PBSA-3% Cloisite 25A (15 min processing time)
D = PBSA-3% Cloisite 25A (20 min processing time)

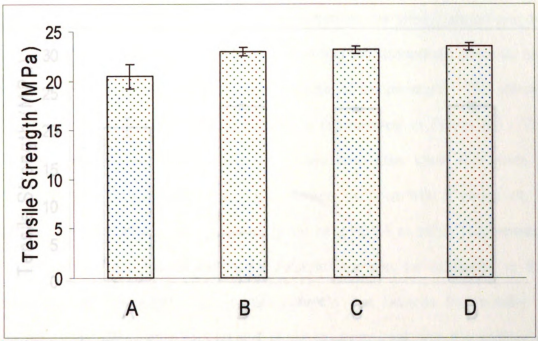

Figure 4.3: *Comparison of tensile strength of PBSA and PBSA-3% Cloisite 25A nanocomposites*

A = PBSA (3 min processing time)
B = PBSA-3% Cloisite 25A (10 min processing time)
C = PBSA-3% Cloisite 25A (15 min processing time)
D = PBSA-3% Cloisite 25A (20 min processing time)

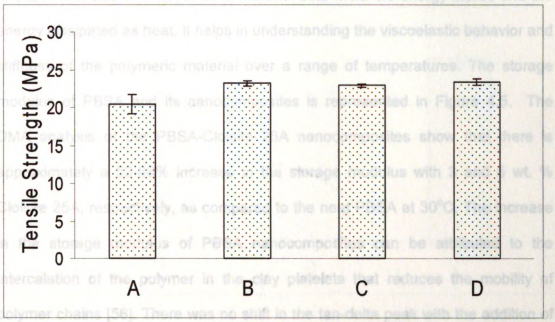

Figure 4.4: *Comparison of tensile strength of PBSA and PBSA-5% Cloisite 25A nanocomposites*

A = PBSA (3 min processing time)
B = PBSA-5% Cloisite 25A (10 min processing time)
C = PBSA-5% Cloisite 25A (15 min processing time)
D = PBSA-5% Cloisite 25A (20 min processing time)

4.1.2 Dynamic Mechanical Analysis: The storage modulus, loss modulus, and tan delta peak were analyzed with the help of the DMA. The storage modulus and loss modulus of a viscoelastic material determine the energy stored and the energy dissipated as heat. It helps in understanding the viscoelastic behavior and stiffness of the polymeric material over a range of temperatures. The storage modulus of PBSA and its nanocomposites is represented in Figure 4.5. The DMA analysis of the PBSA-Cloisite 25A nanocomposites show that there is approximately a 53-88% increase in the storage modulus with 3 and 5 wt. % Cloisite 25A, respectively, as compared to the neat PBSA at 30°C. The increase in the storage modulus of PBSA nanocomposites can be attributed to the intercalation of the polymer in the clay platelets that reduces the mobility of polymer chains [56]. There was no shift in the tan-delta peak with the addition of the organo-clay in the polymer matrix.

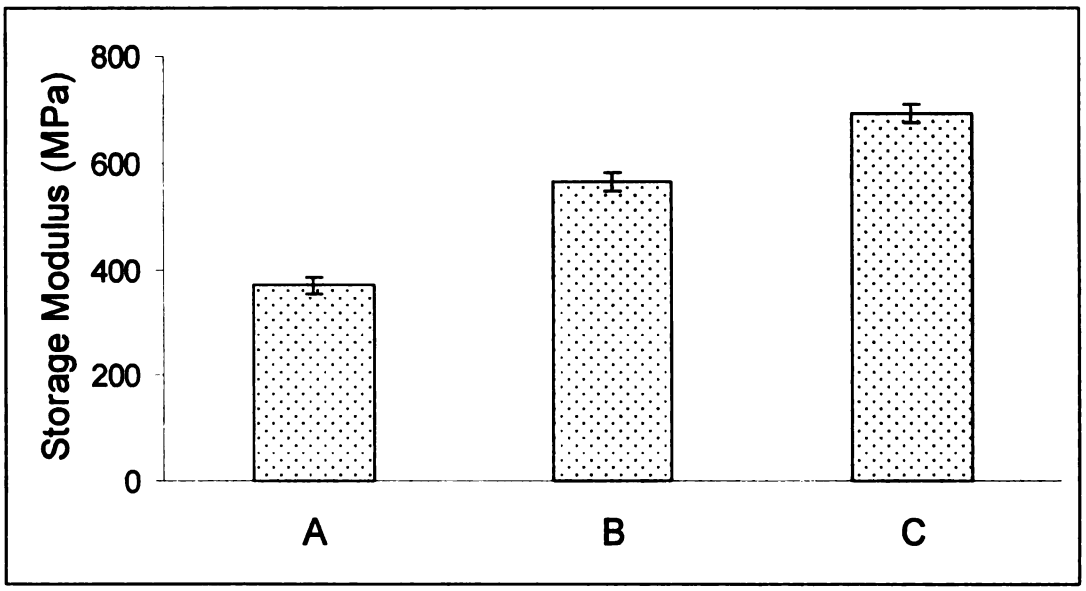

Figure 4.5: *Storage Modulus of PBSA Cloisite 25A nanocomposites*

A = PBSA (3 min processing time)
B = PBSA-3% Cloisite 25A (15 min processing time)
C = PBSA-5% Cloisite 25A (20 min processing time)

4.1.3 Barrier Properties of PBSA Nanocomposites: Evaluation of the barrier properties is crucial for determining the possible food and medical packaging applications of the polymeric material. Poor oxygen gas and water vapor permeability reduce the shelf life of the food or pharmaceutical product by producing physical and chemical changes. Oxidation and loss of crispiness in the food product as well as stability of the pharmaceutical product are some of the common factors which determine the selection of the package system for a particular product. The permeability through the polymer is a combination of three phenomenons: absorbtion, permeation, and desorbtion. Figure 4.6 shows a schematic representation of the permeability mechanism through a polymeric material.

The permeability coefficient (P) of a polymer is defined as the product of a diffusion coefficient (D) and a solubility coefficient (S). PBSA is polar in nature. Therefore, it has a higher water solubility coefficient as compared to polyolefins.

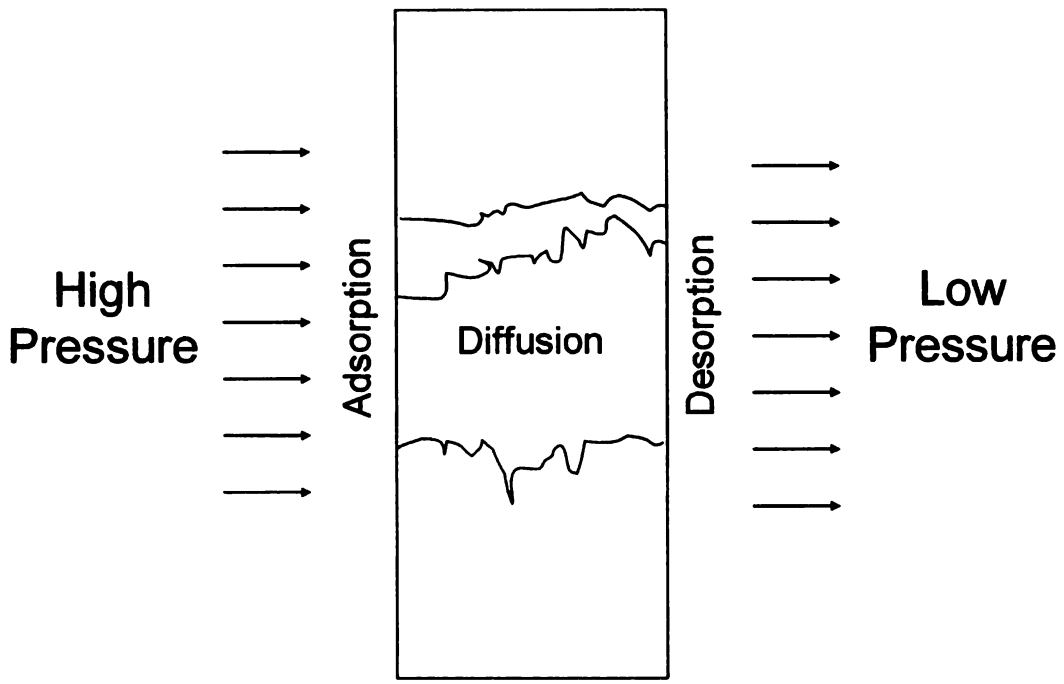

Fig. 4.6: *Permeability Mechanism*

$$P = D \times S$$

4.1.4 Water Vapor Barrier. The permeability of a polymer is the product of diffusion and solubility. The high aspect ratio of the clay combined with the dispersion of the clay and proper orientation of the clay platelets in the polymer matrix help in reducing the diffusion of the water vapors and other permeants. Morphology and chemical structure also affect the barrier properties of a polymer. We used compression-molded PBSA nanocomposites films to evaluate the water barrier properties. The water vapor permeability of PBSA and PBSA-3% Cloisite 25A is represented in Figure 4.7. The water barrier of compression-molded PBSA was found to be poor as compared to commercially available polyethylene. The water vapor barrier of PBSA improved by 70% with the addition of 3 wt.% Cloisite 25A. The improvement in water barrier can be related to the tortuous zig- zag path created by the clay platelets which hindered the diffusion process resulting in the improvement of the water barrier characterstics of the polymer. A schematic representation of the tortuous zig-zag path is shown in Figure 4.8. Ray et. al. [51] observed similar kinds of results for PLA-organically modified clay-based nanocomposites. Processing of the films play an important part in the morphology and the barrier characteristics. Therefore, the permeability of the PBSA nanocomposite films can be improved by preparation of the cast films using biaxial orientation.

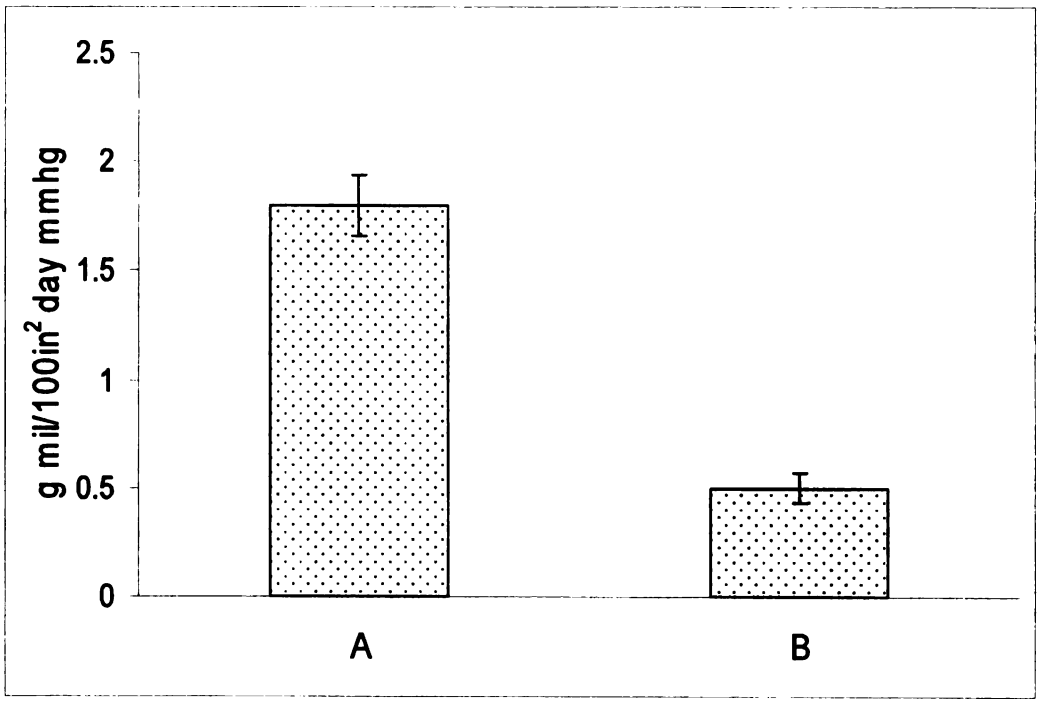

Fig 4.7: *Water vapor permeability of PBSA Cloisite 25A Nanocomposites*

A = PBSA
B = PBSA-3% 25A

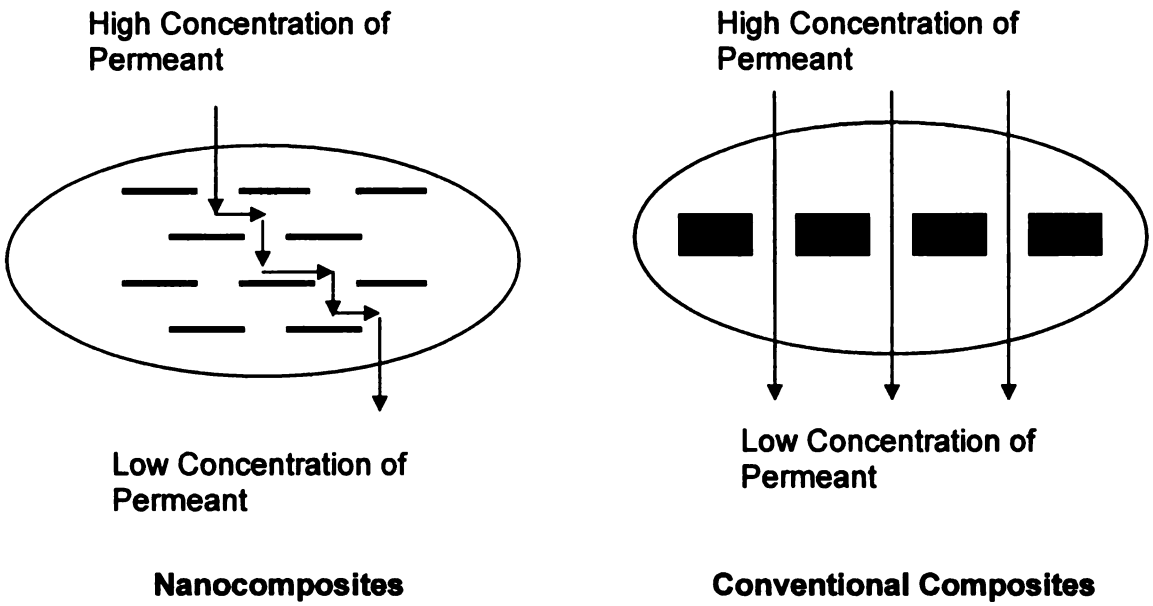

Fig 4.8: *Schematic representation of permeation process: Nano-composites Vs. Conventional composites*

4.1.5 Oxygen Gas Barrier. The oxygen gas permeability coefficients of PBSA, PBSA-3% Cloisite 25A are represented in Figure 4.9. The oxygen barrier of PBSA-3% Cloisite 25A improved by 56% as compared to the neat polymer. The exfoliation of the clay in the PBSA-3% Cloisite 25A is responsible for the creation of the tortuous zig-zag path as explained in Figure 4.8.

Table 4.2. *Barrier Properties of PBSA Nanocomposites*

Material	Water vapor permeability	Oxygen permeability
	(g mil/ 100 in^2 day mmHg)	(cc mil/ 100 in^2 day atm)
PBSA	1.8	80
PBSA-3% Cloisite 25A	0.5	35.5

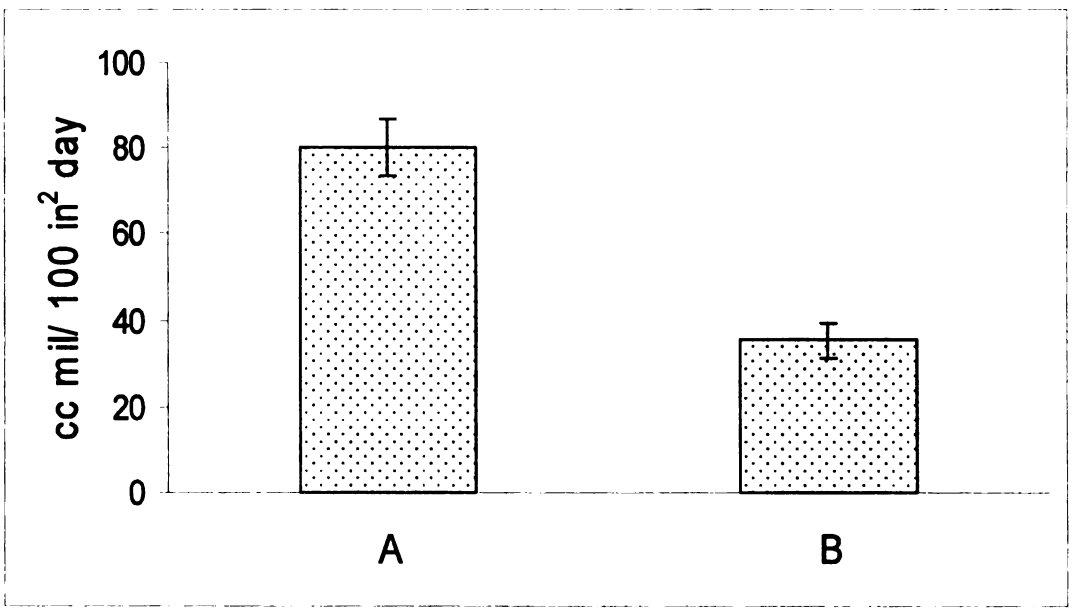

Fig 4.9: *Oxygen gas permeability of PBSA Cloisite 25A Nanocomposites*

A = PBSA
B = PBSA-3% Cloisite 25A

4.1.6 Notched Izod Impact Strength: Izod impact strength plays an important role to select the polymer for particular applications. It helps us to understand the effect of stress concentration at notch on the performance of the polymers. The izod impact strength of PBSA, PBSA-3 wt.% Cloisite 25A and PBSA-5 wt.% Cloisite 25A are represented in Figure 4.10. The impact strength of the PBSA decreased with the addition of the clay in the PBSA matrix. The energy required to break the PBSA specimens was 115 J/m. It was noted that the energy required for the PBSA-3wt.% Cloisite 25A nanocomposites and PBSA-5wt.% Cloisite 25A nanocomposites decreased to about 50 J/m. This indicates that there was more stress concentration in the case of PBSA nanocomposites as compared to the neat polymer.

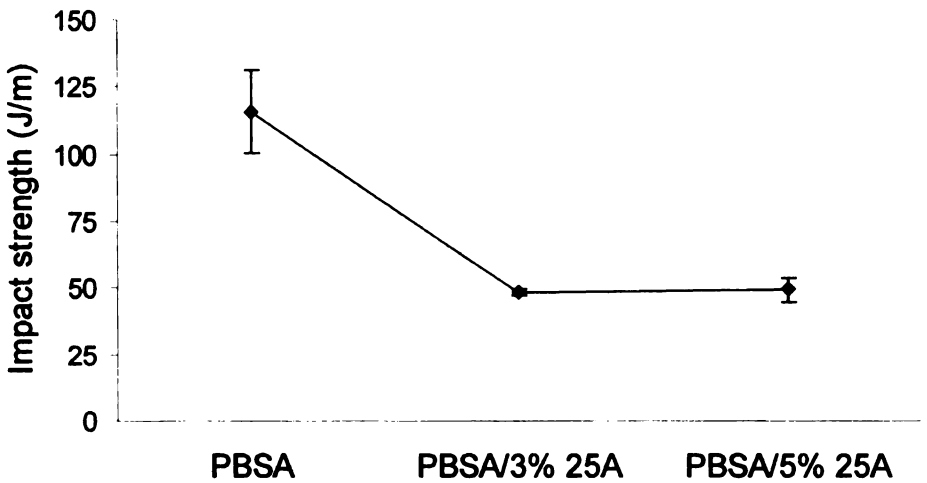

Fig. 4.10: *Izod impact strength of PBSA and PBSA Cloisite 25A nanocomposites*

4.1.7 XRD Analysis. X-ray diffraction (XRD) is widely used to analyze the morphology of polymer–clay nanocomposites. XRD data provides interlayer spacing or d-spacing between the clay platelets. PBSA-3% 25A (15 min. cycle time) and PBSA-5% 25A (20 min. cycle time) have been analyzed at the wavelength of 0.015418 nm. The interlayer spacing of Cloisite 25A, PBSA-3 wt.% Cloisite 25A and PBSA-5wt.% Cloisite 25A are represented in Table 4.3. There was no d_{001} peak in PBSA-3 wt.% w/w 25A which would have indicated the exfoliation of the clay in the polymer matrix. For PBSA-5 wt.% 25A, the interlayer spacing between the clay platelets increased to 34 Å from 18.6 Å. The data supports better dispersion of clay platelets in the polymer matrix at a low weight percentage. The diffractograms of PBSA-3% Cloisite 25A and PBSA-5% 25A are represented in Figure 4.11.

Table 4.3. *Interlayer Spacing or d Spacing of Clay and PBSA Nanocomposites*

Material	Interlayer Spacing (Å)
Cloisite 25A*	18.6
PBSA-3% Cloisite 25A (15 min. cycle time)	No Peak
PBSA-5% Cloisite 25A (20 min. cycle time)	32.1

* Data from the Southern Clay Products, Texas

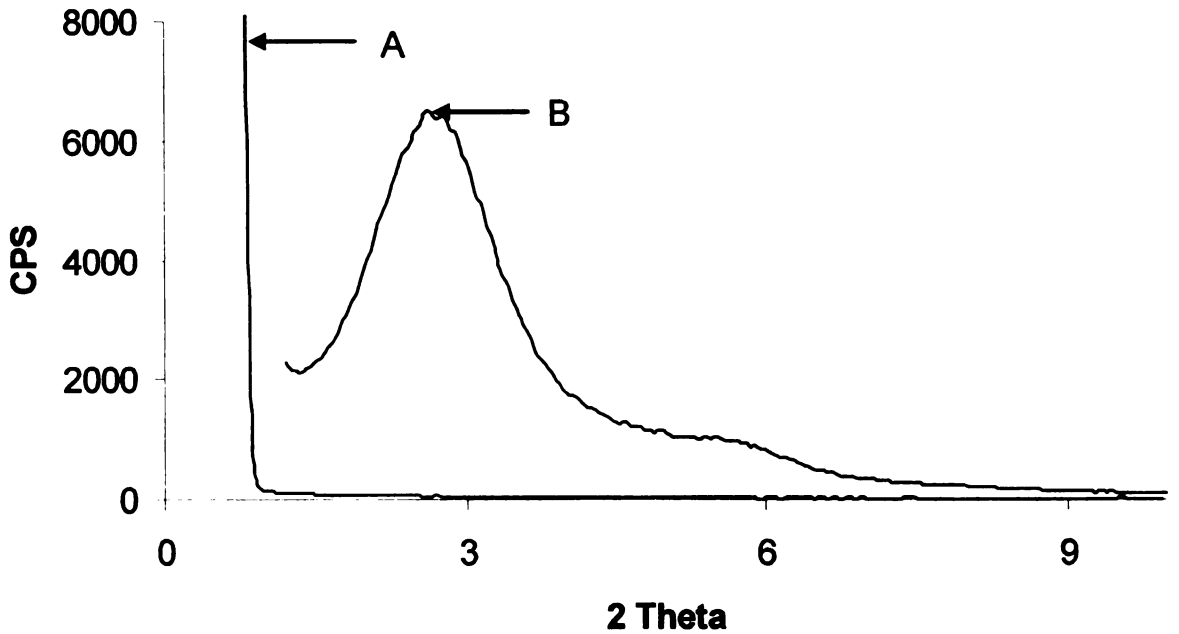

Figure 4.11: *X-Ray Diffractogram of PBSA Cloisite 25A nanocomposites*

A = PBSA-3% Cloisite 25A
B = PBSA-5% Cloisite 25A

4.1.8 Differential Scanning Calorimetry. The total heat of fusion (ΔH_m), calculated by the integration of the area under the melting peak is shown in Table 4.4. The heat of fusion decreased significantly with the incorporation of 3 wt. % Cloisite 25A as compared to the neat PBSA. The morphology of the clay platelets in the polymer matrix also affects the overall crystallization. Krikorian et. al. [76] observed that increased sperulite nucleation is achieved in the intercalated kind of morphology. We observed the exfoliation kind of morphology in the PBSA - 3 wt.% Cloisite 25A system. TEM images and XRD indicate that a combination of intercalation and exfoliation exist in the PBSA-5% Cloisite 25A nanocomposites [76]. The intercalated portion might be responsible for the higher enthalpy of PBSA-5% Cloisite 25A than PBSA-5% Cloisite 25A.

Table 4.4. *Enthalpy of Melting of PBSA Cloisite 25A Nanocomposites*

Material	Enthalpy of melting (J/g)	Standard Deviation
PBSA	50.6	1.1
PBSA-3% Cloisite 25A	36.6	0.8
PBSA-5% Cloisite 25A	39.7	4.4

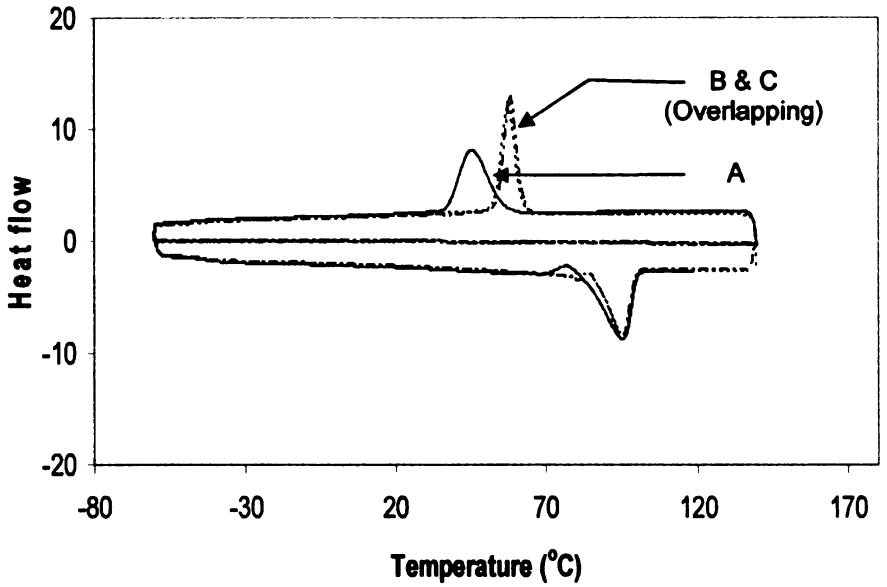

Fig. 4.12 *Thermographs of PBSA Cloisite 25A nanocomposites*

A = PBSA
B = PBSA-3% Cloisite 25A
C = PBSA-5% Cloisite 25A

TEM images:-

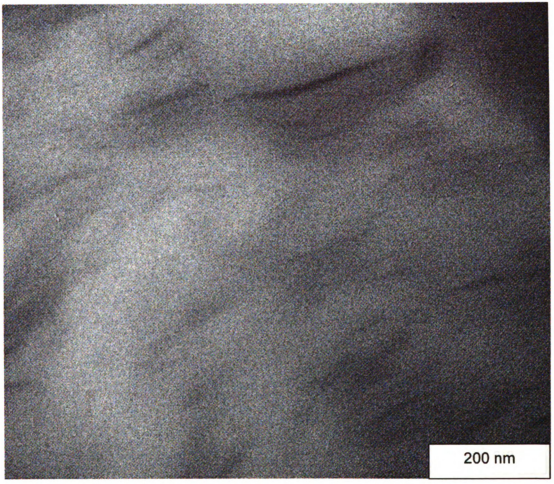

Fig: 4.13: *TEM Photomicrographs of PBSA-3% Cloisite 25A*

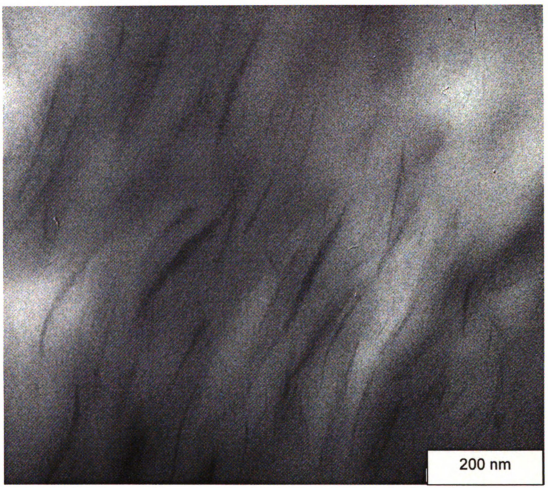

Fig: 4.14: *TEM Photomicrographs of PBSA-5% Cloisite 25A*

Part II

PBS 1020 - Cloisite 25A

Nanocomposites

4.1.9 Tensile Properties of PBS Nanocomposites. The properties of PBS-3% 25A and PBS-5% 25A nanocomposites were studied at processing cycle times of 5 mins., 10 mins. and 15 mins. The mechanical, thermo-mechanical, and barrier properties of PBS nanocomposites were evaluated. The tensile properties of the PBS and PBS nanocomposites were measured as per ASTM D-638. The tensile properties of PBS-3% 25A are represented in Figure 4.15. The PBS 1020 has 300% elongation at break. The elongation of PBS improved by 20% due to the reinforcement of the matrix with 3% Cloisite 25A at a different cycle time.

The increase in the cycle time has no effect on the elongation of PBS-3% Cloisite 25A. This could be explained by the good polymer-nanoclay interaction. The elongation of PBS-5% Cloisite 25A is represented in Figure 4.16. It was also observed that the increase in the clay content from 3% wt.% to 5 wt.% did not help in further improving the tensile properties. The tensile strength of the PBS nanocomposites improved by 10% with the addition of 3% and 5 wt.% organically modified clay. These results support that the 3% Cloisite 25A is optimum for this particular polymer matrix-clay system, and the increase of the clay content to 5 wt. % did not affect the properties of the system.

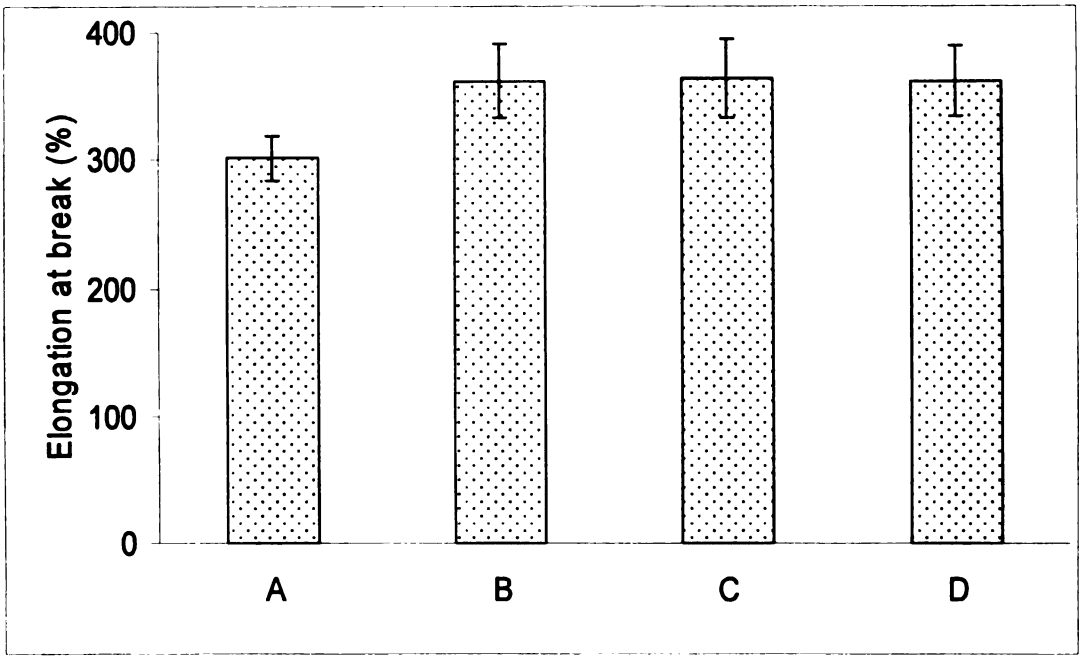

Figure 4.15: *Comparison of percentage elongation of PBS and PBS-3% Cloisite 25A nanocomposites*

A = PBS (3 min processing time)
B = PBS-3% Cloisite 25A (5 min processing time)
C = PBS-3% Cloisite 25A (10 min processing time)
D = PBS-3% Cloisite 25A (15 min processing time)

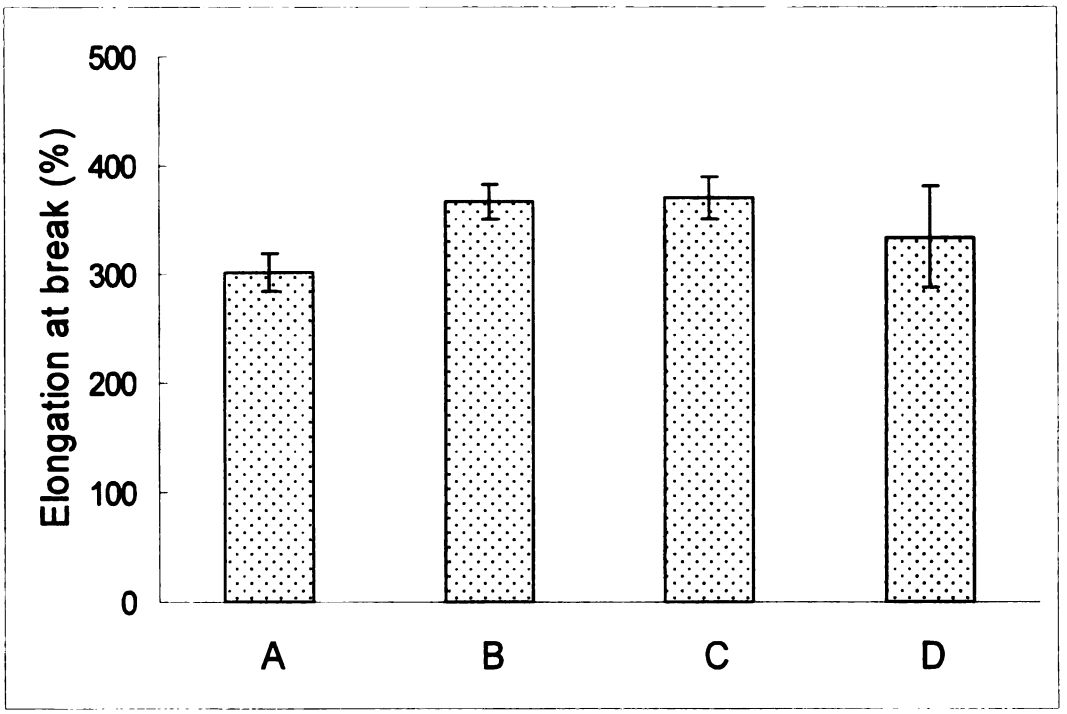

Figure 4.16: *Comparison of percentage elongation of PBS and PBS-5% Cloisite 25A nanocomposites*

A = PBS (3 min processing time)
B = PBS-5% Cloisite 25A (5 min processing time)
C = PBS-5% Cloisite 25A (10 min processing time)
D = PBS-5% Cloisite 25A (15 min processing time)

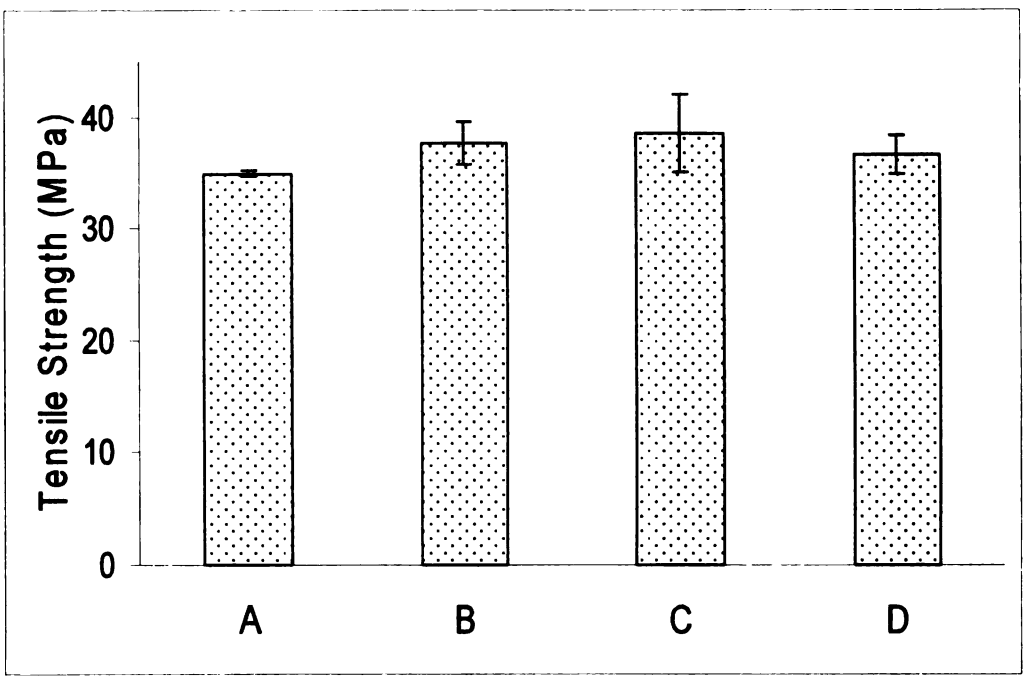

Figure 4.17: *Comparison of tensile strength of PBS and PBS-3% Cloisite 25A nanocomposites*

A = PBS (3 min processing time)
B = PBS-3% Cloisite 25A (5 min processing time)
C = PBS-3% Cloisite 25A (10 min processing time)
D = PBS–3% Cloisite 25A (15 min processing time)

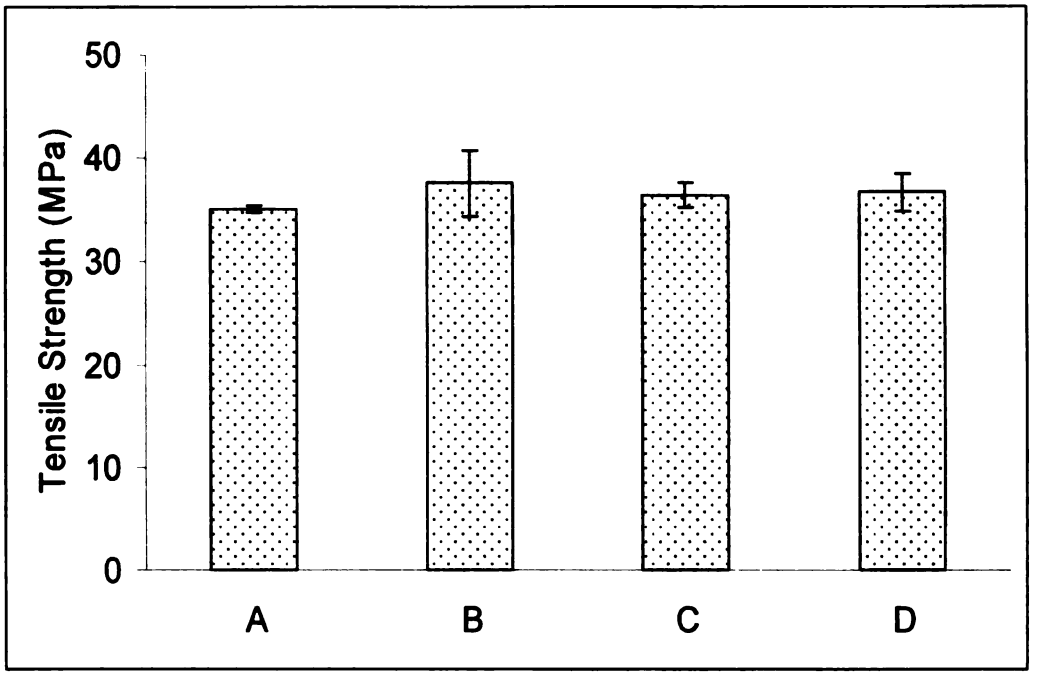

Figure 4.18: *Comparison of tensile strength of PBS and PBS-5% Cloisite 25A nanocomposites*

A = PBS (3 min processing time)
B = PBS-5% Cloisite 25A (5 min processing time)
C = PBS-5% Cloisite 25A (10 min processing time)
D = PBS-5% Cloisite 25A (15 min processing time)

4.1.10 Storage Modulus. The storage modulus was measured with the help of DMA Q800. The data is represented in Figure 4.19. The storage modulus of the PBS increased with the increasing nano-clay content in the polymer matrix. The modulus of the PBS matrix increased by 30% and 57% with loadings of 3% and 5 wt % clay, respectively. The organo-clay platelets can reduce the mobility of the polymer chains as well as increase the reinforcement of the polymer matrix. The increase in the storage modulus in the PBS clay nanocomposites has also been reported by other researchers.

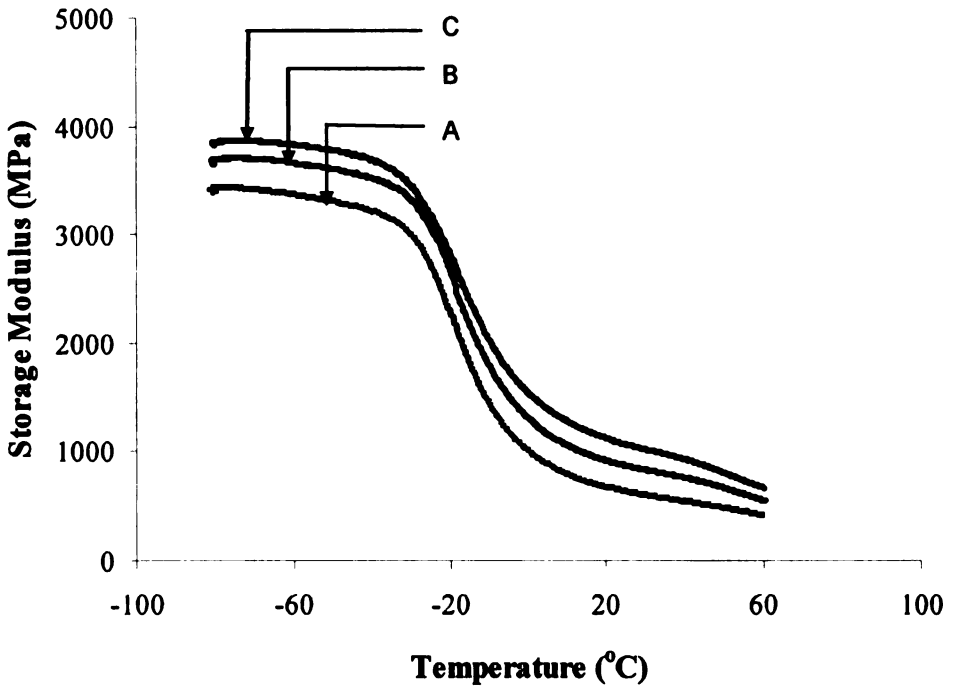

Fig. 4.19: *Graph of Storage Modulus of PBS Cloisite 25A nanocomposites*

A = Neat PBS
B = PBS-3% Cloisite 25A processed for 5 minute
C = PBS-5% Cloisite 25A processed for 5 minute

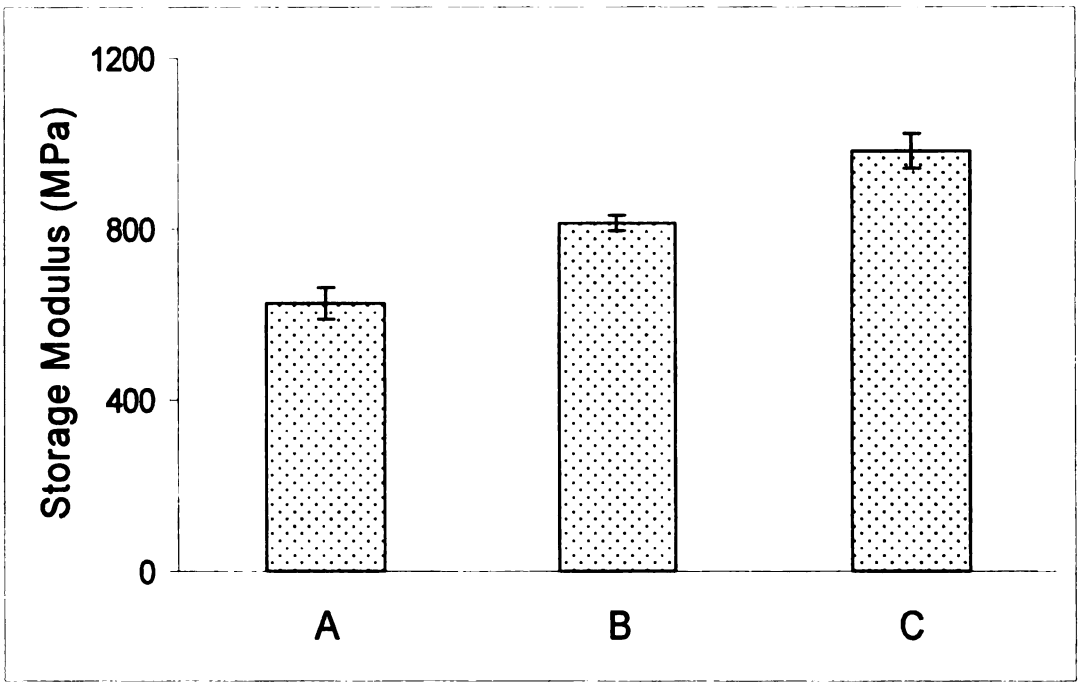

Figure 4.20: *Storage modulus of PBS Cloisite 25A nanocomposites*

A = PBS
B = PBS-3% Cloisite 25A
C = PBS-5% Cloisite 25A

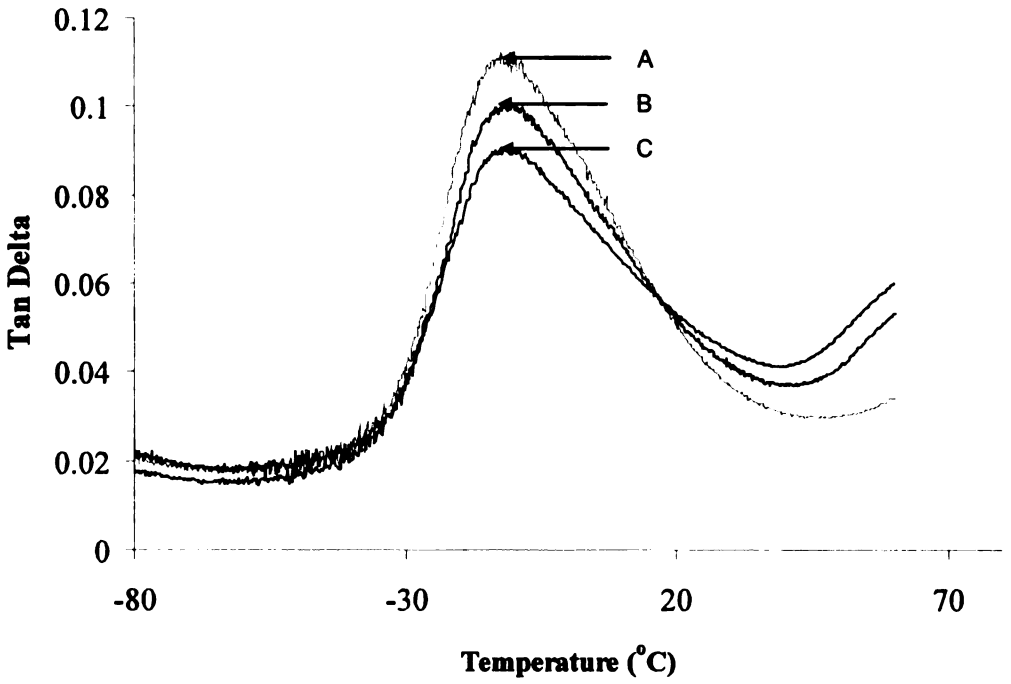

Figure 4.21: *Tan δ of PBS Cloisite 25A nanocomposites*

A=PBS (3 min processing time)
B=PBS-3% Cloisite 25A (5 min processing time) at 160°C
C=PBS-5% Cloisite 25A (5 min processing time) at 160°C

4.1.11 Permeability: Free volume of a polymer, orientation of polymer chains, and the percentage crystallinity of the polymeric materials play an important part in understanding the permeability of a packaging material. For the polymer-clay nanocomposites system, the clay platelets hinder the crystallinity of the polymer nanocomposites by reducing the flexibility of the chains because of the intercalation of the polymer between the clay platelets. The high aspect ratio and the tortuous path created by the layered silicates are some of the factors responsible for reducing the permeability of the polymer. Therefore, the dispersion of the clay in the polymer matrix plays a crucial role in reducing the permeability. The permeability of compression molded films of PBS-3 wt.% 25A and PBS-5 wt.% 25A nanocomposites were evaluated at the 5-minute processing cycle time. The permeability of the nanocomposites decreased as compared to the virgin polymer because layered silicate platelets hindered the permeability by creating a "tortuous path" which decreased the transmission rate of the water vapors and gases.

4.1.12 Water Vapor Permeability. The water vapor permeability of PBS, PBS-3% 25A (5 mins.) and PBS-5% 25A (5 mins.) is represented in Figure 4.22. The permeability of PBS-3% 25A decreased by 20% as compared to the neat PBS polymer. The increase in the clay content from 3 wt. % to 5 wt. % did not help in reducing the permeability of the polymer. The increase in the clay content to 5% may have reduced the crystallinity process of the polymer-clay nanocomposites

that may have compensated for the barrier created by the increase in the layered silicates.

The Neilson model is a two-dimensional model that predicts the permeability of the polymer composites. This model assumes that the clay platelets are dispersed parallel to the film surface. The mathematical equation for the Neilson model is [29, 51]:

$$P_N/P_P = V_P / 1 + (L/2W) V_F$$

Where,
P_N = Permeability of the composites
P_P = Permeability of the polymer
V_P= Volume fraction of the polymer
V_F= Volume fraction of the filler
L/W = Aspect ratio of the filler

Cloisite 25A has an aspect ratio of 200 (approx.). We observed that water vapor permeability values obtained for the PBS-3 wt. % nanocomposites match the aspect ratio value of 150. The TEM images of the PBS-nanocomposite support the aspect ratio of 150. However, no further increase was observed in the permeability of the PBS nanocomposites with elevated clay content from 3 wt. % to 5 wt. %. This can be explained by the partial agglomeration of clay platelets in the polymer matrix as observed in the TEM images.

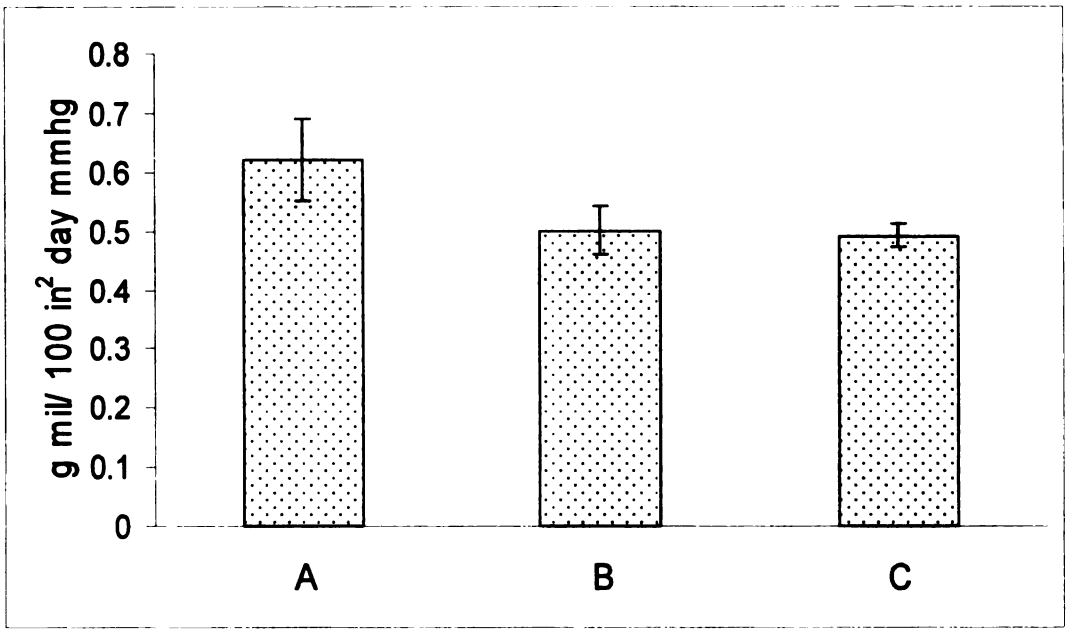

Fig 4.22: *Water vapor permeability of PBS-3% 25A and PBS-5% 25A processed at 5 min. cycle time*

A = PBS
B = PBS-3% Cloisite25A
C = PBS-5% Cloisite25A

4.1.13 Oxygen Permeability: The oxygen gas permeability of PBS, PBS-3% 25A, and PBS-5% 25A are represented in Figure 4.23. We observed around 5% improvement in the oxygen barrier with the addition of 3 wt. % organo-clay. The addition of 5 wt. % organo-clay in the polymer matrix increased the permeability of the PBS-nanocomposites. This could be explained by the agglomeration of clay in the polymer matrix at a high clay concentration.

Table 4.5. *Barrier Properties of PBS Cloisite 25A Nanocomposites*

Material	Water Vapor Permeability (g mil/ 100 in^2 day mmhg)	Oxygen Permeability (cc mil/ 100 in^2 day atm)
PBS	0.62	30.82
PBS-3% Cloisite 25A	0.5	29.34
PBS-5% Cloisite 25A	0.49	42.9

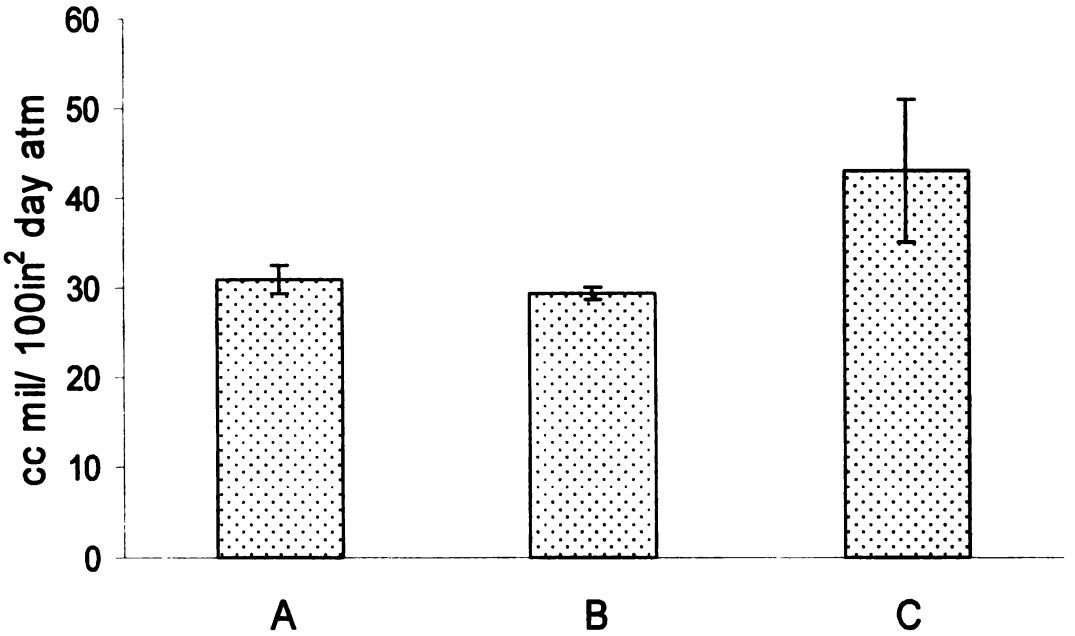

Fig: 4.23: *Oxygen gas permeability of PBS and PBS nanocomposites*

A = PBS (3 min processing time)
B = PBS-3% Cloisite 25A (5 min processing time)
C = PBS-5% Cloisite 25A (5 min processing time)

4.1.14 Differential Scanning Calorimetry. The total heat of fusion (ΔH_m) calculated by the integration of the area under the melting peak and crystallization onset temperatures are shown in Table 4.6. A decrease was observed in the crystallization onset temperature in the presence of the Cloisite® 25A. The heat of fusion increases upon the incorporation of 3 wt. % Cloisite 25A as compared to the neat PBS. However, the heat of fusion of PBS-3 wt. % Cloisite 25A and PBS-5 wt. % Cloisite® 25A are almost similar. This can be ascribed to the phenomenon that a small amount of clay can increase the rate of crystallization; however, high organoclay loading reduces the rate of crystallization. The morphology of the clay platelets in the polymer matrix also affects the overall crystallization. Krikorian et. al [76] observed that increased sperulite nucleation is achieved in the intercalated kind of morphology. A combination of exfoliation and interaction morphology was observed in the PBS-3% w/w Cloisite® 25A system; whereas TEM images and XRD support the combination of intercalation and partial agglomeration in the PBS - 5% 25A nanocomposites.

Table 4.6. *Enthalpy of Melting of PBS Cloisite 25A Nanocomposites*

Material	Enthalpy of Melting (J/g)	Standard Deviation
PBS	53.3	4.8
PBS-3% Cloisite 25A	55.3	0.9
PBS-5% Cloisite 25A	55.6	2.2

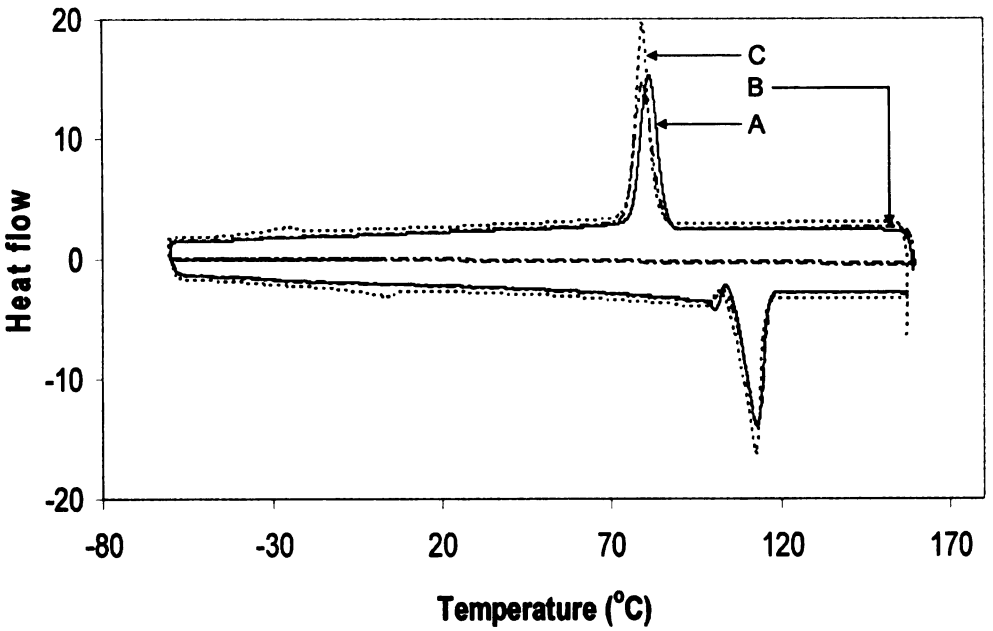

Fig. 4.24 *Thermographs of PBS Cloisite 25A nanocomposites*

A = PBS
B = PBS-3% Cloisite25A
C = PBS-5% Cloisite 25A

4.1.15 XRD Analysis: The X-ray diffraction of PBS-3% 25A (5-min. cycle time) and PBS-5% 25A (5-min. cycle time) has been studied at the wavelength of 0.015418 nm. The gallery spacing (d_{001} spacing) between the clay platelets of PBS-3% 25A and PBS-5% 25A nanocomposites when calculated through bragg's equation is 35.4 and 34.6 A, respectively. The increase in the interlayer spacing supports the intercalated morphology in the PBS-3 wt. % 25A and PBSA-5 wt. % nanocomposites.

Table 4.7. *Interlayer Spacing of PBS-3% 25A (5 mins.) and PBS-5% 25A (5 mins.)*

Material	Interlayer Spacing (Å)
Cloisite 25A*	18.6
PBS-3% Cloisite 25A	35.34
PBS-5% Cloisite 25A	34.65

* Data from the Southern Clay Products, Texas

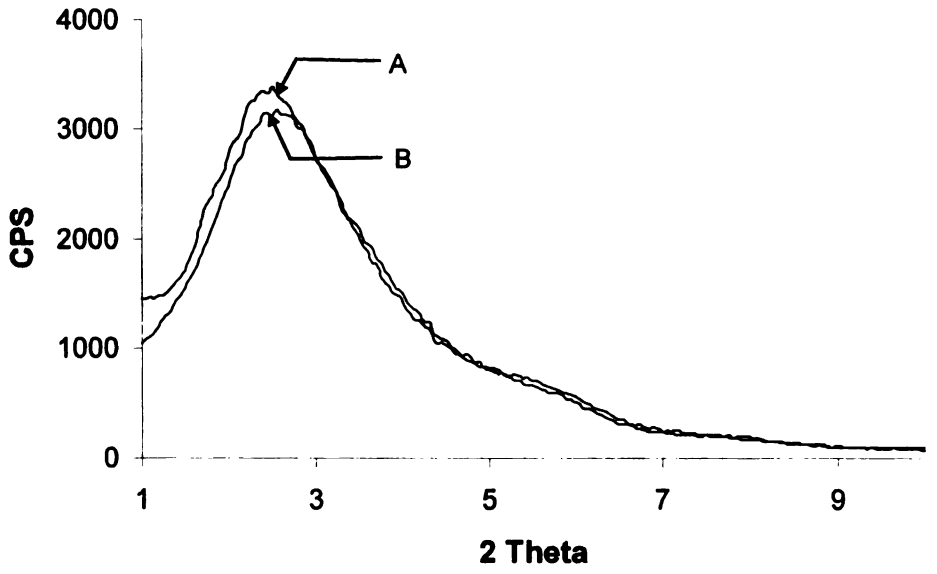

Fig. 4.25 *XRD Analysis of PBS-3% Cloisite 25A and PBS-5% Cloisite 25A Processed at 5-min. cycle time*

A = PBS-3% Cloisite 25A
B = PBS-5% Cloisite 25A

4.1.16 TEM Studies: Figures 4.26 and 4.27 represent TEM photo micrographs of PBS-3% wt.% Cloisite 25A and PBS-5 wt.% Cloisite 25A nanocomposites, respectively. An exfoliated type of morphology was obtained in the PBS-3 wt.% Cloisite 25A nanocomposites while a combination of intercalated and exfoliated type of morphology was observed in PBS-5 wt.% Cloisite 25A.

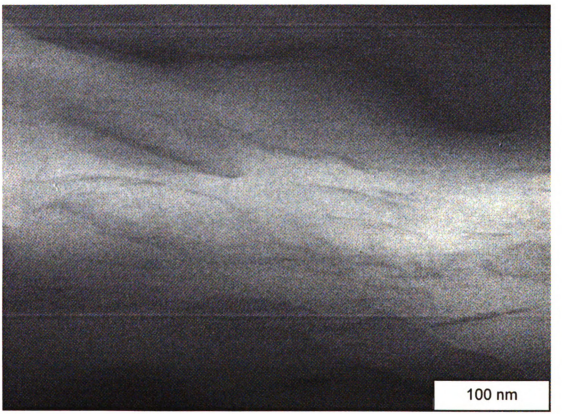

Fig: 4.26: *TEM Photomicrographs of PBS- 3% Cloisite 25A processed at 5 minute cycle time.*

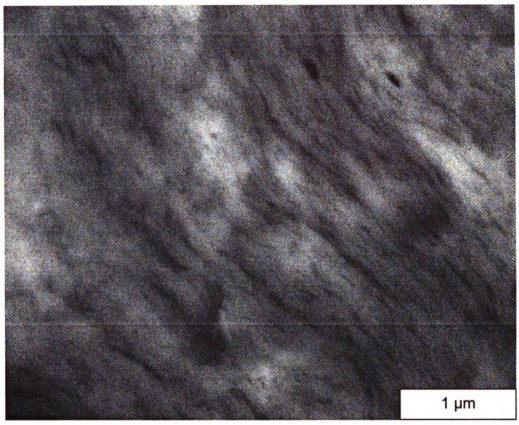

Fig: 4.27: *TEM Photomicrographs of PBS- 5% Cloisite 25A processed at 5 minute cycle time.*

Chapter 5

Conclusion and Recommendation for Future Work

We have successfully developed biodegradable poly(butylene succinate)-Cloisite 25A (OMMT) nanocomposites. The effect of variation in the processing conditions, especially processing cycle time on the mechanical properties, was studied. It was observed that the higher processing time can help in the improvement of the mechanical properties of the polymer.

Significant improvement was observed in the storage modulus and thermo-mechanical properties. The storage modulus of PBSA-5% Cloisite 25A improved by 87% as compared to virgin PBSA. The storage modulus of PBS-5% Cloisite 25A increased by 57% as compared to the neat polymer. The layered silicates created a tortuous zig-zag path for the permeant which help with the water and oxygen gas barrier properties of PBSA-Cloisite 25A and PBS-Cloisite 25A nanocomposites. The oxygen and water vapor barrier of PBSA improved by 52% and 76%, respectively, with 5% wt.% Cloisite 25A. A 20% improvement was observed in the water vapor barrier properties of PBS nanocomposites. There

was XRD, and TEM revealed the intercalated and exfoliated kind of morphology in the PBS and PBSA nanocomposites.

In conclusion:

a. Increase in the processing cycle time helped in the better dispersion and exfoliation of the clay in the polymer matrix of PBSA-Cloisite 25A nanocomposites.

b. The reinforcement of the PBS and PBSA with Cloisite-25A helped in increasing the stiffness of the polymer.

c. PBS nanocomposites and PBSA nanocomposites possess better thermo-mechanical properties as compared to respective virgin polymers.

d. Barrier properties of PBS-Cloisite 25A nanocomposites and PBSA-Cloisite 25A nanocomposites improved significantly because of the creation of a tortuous zig-zag path by the clay platelets in the polymer matrix.

e. There was no significant difference in the properties of PBS-3 wt.% Cloisite 25A and PBS-5 wt. % Cloisite 25A. Therefore, it is perhaps safe to conclude that 3 wt% Cloisite 25A concentration can be the optimum amount of clay in the PBS nanocomposites under the present experimental set of conditions or parameters.

f. XRD, TEM, and properties correlation were well established.

g. The increase in the processing cycle time from 5 mins. to 15 mins. did not have much impact on tensile properties of PBS-3% 25A.

h. Based on our studies, it is recommended that these studies be further extended by utilizing the Twice Functionalized Clay (TFC)

i. The stiffness of PBS and PBSA can be enhanced by preparing blends with stiff materials such as Sorona™.

j. The compression molding technique was used to prepare nanocomposites films. Better PBS and PBSA nanocomposite properties can be obtained through extrusion-blown film or biaxial cast film production because of orientation of the polymeric chain. Therefore, this work can be extended by producing nanocomposites film at blown film or cast film extruder.

k. Nano-reinforcement helps in improving processing conditions. Therefore, the effect of nano-reinforcement on the processing properties of PBS and PBSA can be evaluated.

REFERENCES:

1. Shih-Jung liu, Ming-Jen Lin, and Yi-Chuan Wu, *An Experimental Study of the Water-Assisted Injection Molding of Glass Fiber Filled poly-butylene-terephthalate (PBT) Composites. COMPOSITES SCIENCE AND TECHNOLOGY*, 2007. **67**: p. 1415.

2. J. Lange, and Y. Wyser, *Recent Innovations in Barrier Technologies for Plastics Packaging – a Review. PACKAGING TECHNOLOGY AND SCIENCE*, 2003. **16**: p. 149.

3. R.A. Gross, and B. Kalra, *Biodegradable Polymers for the Environment. SCIENCE*, 2002. **297**(2): p. 803.

4. R.A. Auras, B. Harte, and S. Selke, *Poly(Lactic Acid) Films as Food Packaging Materials. JOURNAL OF APPLIED POLYMER SCIENCE*, 2004. **92**(3): p. 1790.

5. A.K. Mohanty, M. Misra, and G. Hinrichsen *Biofibres, Biodegradable Polymers and Biocomposites: An Overview. MACROMOLECULAR MATERIALS AND ENGINEERING*, 2000. **1**(24): p. 276.

6. Long Jiang, Michael P. Wolcott, and Jinwen Zhang, *Study of Biodegradable Polylactide/ Poly(butylene adipate-co-terephthalate) Blends Biomacromolecules*, 2006 **7** p. 199.

7. Jong-Whan Rhim, and Perry K.W. Ng; *Natural Biopolymer-Based Nanocomposite Films for Packaging Applications. CRITICAL REVIEWS IN FOOD SCIENCE AND NUTRITION*, 2007(47): p. 411

8. S. Philip, T. Keshavarz, and I. Roy, *Review Polyhydroxyalkanoates: Biodegradable Polymers with a Range of Applications. JOURNAL OF CHEMICAL TECHNOLOGY AND BIOTECHNOLOGY*, 2007. **82**: p. 233.

9. Ying Zheng, Ernest K. Yanful, and Amarjeet S. Bassi, *A Review of Plastic Waste Biodegradation. CRITICAL REVIEWS IN BIOTECHNOLOGY*, 2005. **25**: p. 243.

10. R.A. Shanks, A. Hodzic, and D. Ridderhof, *Composites of Poly(lactic acid) with Flax Fibers Modified by Interstitial Polymerization. JOURNAL OF APPLIED POLYMER SCIENCE*. **99**(5): p. 2305.

11. *"Techno-economic Feasibility of Large-scale Production of Bio-based Polymers in Europe (PRO-BIP)"; Institute for Prospective Technological Studies, Sevilla, Spain. Website link: accessed on 25 May, 2006: http://www.biomatnet.org/publications/1944rep.pdf*

12. M.K. Akkapeddi, *Glass Fiber Reinforced Polyamide-6 Nanocomposites. POLYMER COMPOSITES*, 2000. **21**(4): p. 576.

13. F.G. Torres and S.F. Bush, *Sheet Extrusion and Thermoforming of Discrete Long Glass Fiber Reinforced Polypropylene. COMPOSITES PART A*, 2000. **31**: p. 1289.

14. Hongzhou Li, Yuxi Jia, Geni Mamtiminc, Wei Jiang, and Lijia An, *Stress Transfer and Damage Evolution Simulations of Fiber-reinforced Polymer-matrix Composites, MATERIALS SCIENCE AND ENGINEERING A.* 2006. **425**: p. 178.

15. K. Senthil Kumar, Naresh Bhatnagar, and Anup K. Ghosh, *Development of Long Glass Fiber Reinforced Polypropylene Composites: Mechanical and Morphological Characteristics. JOURNAL OF REINFORCED PLASTICS AND COMPOSITES*, 2007. **26**(3).

16. Wanjun Liu, Amar K. Mohanty, Lawrence T. Drzal, Manjusri Misra, Joseph V. Kurian, Ray W. Miller, and Nick Strickland, *Injection Molded Glass Fiber Reinforced Poly(trimethylene terephthalate) Composites: Fabrication and Properties Evaluation. Ind. Eng. Chem. Res.*, 2005. **44**: p. 857.

17. Z.A. Mohd Ishak, Y.W. Leong, M. Steeg, and J. Karger-Kocsis, *Mechanical Properties of Woven Glass Fabric Reinforced in Situ polymerized Poly(butylene terephthalate) Composites. COMPOSITES SCIENCE AND TECHNOLOGY,* 2007. **67**: p. 390.

18. Rahul Bhardwaj, Amar K. Mohanty, L. T. Drzal, F. Pourboghrat, and M. Misra, *Renewable Resource-Based Green Composites from Recycled Cellulose Fiber and Poly(3-hydroxybutyrate-co-3-hydroxyvalerate) Bioplastic. BIOMACROMOLECULES*, 2006. **7**(6): p. 2044.

19. A.K. Mohanty, Mubarak A. Khan, S. Sahoo, and G. Hinrichsen, *Effect of Chemical Modification on the Performance of Biodegradable Jute Yarn-Biopol Composites. JOURNAL OF MATERIALS SCIENCE* 2000. **35**: p. 2589.

20. A.K. Mohanty, M. Misra, and L. T. Drzal, *Sustainable Bio-Composites from Renewable Resources: Opportunities and Challenges in the Green Materials World. JOURNAL OF POLYMERS AND THE ENVIRONMENT*, 2002. **10**: p. 19.

21. M.S. Huda, A.K. Mohanty, L.T. Drzal, E. Schut, and M. Misra *"Green" composites from recycled cellulose and poly(lactic acid): Physico-*

mechanical and Morphological Properties Evaluation. JOURNAL OF MATERIALS SCIENCE, 2005(40): p. 4221.

22. Peng Ye, Lauren Reitz, Chris Horan, and Richard Parnas, *Manufacture and Biodegradation of Wheat Composite Material. JOURNAL OF POLYMERS AND THE ENVIRONMENT*, 2006. **14**(1).

23. Wanjun Liu, Lawrence T. Drzal, Amar K. Mohanty, and Manjusri Misra, *Influence of Processing methods and Fiber Length on Physical Properties of Kenaf Fiber Reinforced Soy Based Biocomposites. COMPOSITES: PART B*, 2007. **38**: p. 352.

24. D.P. Miller, J.J. Lannutti, and R. D. Noebe, *Fabrication and Properties of Functionally Graded NiAl/Al2O3 Composites. JOURNAL OF MATERIAL RESOURCES,* 1993. **8**(8).

25. Sanjeev Singh, and A.K. Mohanty, *Wood fiber reinforced bacterial bioplastic composites: Fabrication and performance evaluation. COMPOSITES SCIENCE AND TECHNOLOGY*, 2007. **67**: p. 1753.

26. Deborah F. Eckel, Michael P. Balogh, Paula D. Fasulo, and William R. Rodgers, *Assessing Organo-Clay Dispersion in Polymer Nanocomposites. JOURNAL OF APPLIED POLYMER SCIENCE*, 2004. **93**: p. 1110.

27. *Website of Institute of Nanotechnology, UK* http://www.nano.org.uk/whatis.htm *accessed 10 July, 2006.*

28. E. Picard, H. Gauthier, J.F. Gerard, and E. Espuche, *Influence of the intercalated Cations on the Surface Energy of Montmorillonites: Consequences for the Morphology and Gas Barrier Properties of Polyethylene/Montmorillonites Nanocomposites. JOURNAL OF COLLOID AND INTERFACE SCIENCE,* 2007. **307** p. 364.

29. Kazuhisa Yano, Arimitsu Usuki, and Akane Okada, *Synthesis and Properties of Polyimide-Clay Hybrid Films. JOURNAL OF POLYMER SCIENCE PART A: POLYMER CHEMISTRY*, **35**(11): p. 2289.

30. Margarita Darder, Pilar Aranda, and Eduardo Ruiz-Hitzky, *Bionanocomposites: A New Concept of Ecological, Bioinspired, and Functional Hybrid Materials. ADVANCED MATERIALS,* 2007 19 : p 1309.

31. Emmanuel P. Giannnelis, *Polymer Layered SIlicate Nanocomposites. ADVANCED MATERIAL,* 2004 **8** (1): p 29.

32. Suprakas Sinha Ray, and Mosto Bousmina, Progress in Materials Science *Biodegradable Polymers and Their Layered Silicate Nanocomposites: in Greening the 21st Century Materials World,* 2005. **50**: p. 962.

33. Gunter Beyer, *Flame Retardancy of Thermoplastic Polyurethane and Polyvinyl Chloride by Organoclays. JOURNAL OF FIRE SCIENCE*, 2007. **25**: p.65

34. G. Guo, C.B. Park, Y.H. Lee, Y.S. Kim and M. Sain, *Flame Retarding Effects of Nanoclay on Wood-Fiber Composites. POLYMER ENGINEERING AND SCIENCE.* **47**(3): p. 330.

35. Huaili Qina, Quansheng Sub, Shimin Zhang, Bin Zhaoa, and Mingshu Yanga, *Thermal Stability and Flammability of Polyamide 66/Montmorillonite Nanocomposites Polymer*, 2003. **44**(24): p. 7533.

36. Kadhiravan Shanmuganathan, Sarang Deodhar, Nicholas Dembsey, Qinguo Fan, Paul D. Calvert, Steven B. Warner, and Prabir K. Patra, *Flame Retardancy and Char Microstructure of Nylon-6/Layered Silicate Nanocomposites. JOURNAL OF APPLIED POLYMER SCIENCE*, 2007. **104**: p. 1540.

37. Renata Barbosa, Edcleide M. Araújo, Tomas Jeferson A. Melo, and Edson N. Ito, *Comparison of Flammability Behavior of Polyethylene/Brazilian Clay Nanocomposites and Polyethylene/flame Retardants. MATERIALS LETTERS* ***61***, 2007: p. 2575.

38. Arief C. Wibowo, Manju Misra, Hwan-Man Park, Lawrence T. Drzal, Richard Schalek, and Amar K. Mohanty, *Biodegradable Nanocomposites from Cellulose Acetate: Mechanical, Morphological, and Thermal Properties. COMPOSITES: PART A,* 2005.

39. Smita Mohanty, and Sanjay K. Nayak, *Effect of Clay Exfoliation and Organic Modification on Morphological, Dynamic Mechanical, and Thermal Behavior of Melt-Compounded Polyamide-6 Nanocomposites. POLYMER COMPOSITES,* **28**(2): p. 153.

40. Suprakas Sinha Ray, Kazunobu Yamada, Masami Okamoto, and Kazue Ueda, *Polylactide-Layered Silicate Nanocomposite: A Novel Biodegradable Material. NANO LETTERS*, 2002. **2**(10): p. 1093.

41. Yoshihiro Someya, Toshiyuki Nakazato, Naozumi Teramoto, and Mitsuhiro Shibata, *Thermal and Mechanical Properties of Poly(butylene succinate) Nanocomposites with Organo-Modified Montmorillonites. JOURNAL OF APPLIED POLYMER SCIENCE*, 2004. **91**: p. 1463.

42. Arimitsu Usuki, Masaya Kawasumi, Yoshitsugu Kojima, Akane Okada, Toshio Kurauchi, and Osami Kamigaito, *Swelling Behavior of Montmorillonite Cation Exchanged for o) -Amino Acids by e-Caprolactam. JOURNAL OF MATERIAL RESEARCH,* 1993. **8**(5): p.1174.

43. Arimitsu Usuki, Yoshitsugu Kojima, Masaya Kawasumi, Akane Okada, Yoshiaki Fukushima, Toshio Kurauchi, and Osami Kamigaito, *Synthesis of Nylon 6-Clay Hybrid. JOURNAL OF MATERIAL RESEARCH*, 1993. **8**(5): p.1179.

44. Cher H. Davis, Lon J. Mathias, Jeffrey W. Gilman, David A. Schiraldi, J. Randy Shields, Paul Trulove, Tom E. Sutto, and Hugh C. Delong, *Effects of Melt-Processing Conditions on the Quality of Poly(ethylene terephthalate) Montmorillonite Clay Nanocomposites. JOURNAL OF POLYMER SCIENCE PART B: POLYMER PHYSiCS*. **40**: p. 2661.

45. J. Karger-Kocsis, O. Gryshchuk, J. Frohlich, and R. Mulhaupt, *Interpenetrating Vinylester/epoxy Resins Modified with Organophilic Layered Silicates.COMPOSITES SCIENCE AND TECHNOLOGY*, 2003. **63**(14): p. 2045.

46. L.A.S de A. Prado, C.S. Karthikeyan, K. Schulte, S. P. Nunes, Iris L. de Torriani, *Organic Modification of Layered Silicates: Structural and Thermal Characterizations. JOURNAL OF NON CRYSTALLINE SOLIDS*, 2005. **351**(12-13): p. 970.

47. Shaohui Wang, Yong Zhang Zonglin Peng Yinxi Zhang, *New Method for Preparing Polybutadiene Rubber/Clay Composites. JOURNAL OF APPLIED POLYMER SCIENCE*, 2005. **98**(1): p. 227.48. Yoshitsugu Kojima, Arimitsu Usuki, Masaya Kawasumi, Akane Okada, Yoshiaki Fukushima, Toshio Kurauchi, and Osami Kamigaito, *Mechanical Properties of Nylon 6-Clay Hybrid. JOURNAL OF MATERIAL RESEARCH*, 1993. **8**(5): p. 1187.

49. Maged A. Osman, Jorg E. P. Rupp, *Interfacial Interactions and Properties of Polyethylene-Layered Silicate Nanocomposites. MACROMOLECULAR RAPID COMMUNICATIONS*, 2005. **26**: p. 880.

50. T.J. Pinnava, and G.W. Beall, Chapter: *New Conceptual Model for Interpreting Nanocomposite Behavior. POLYMER-CLAY NANOCOMPOSITES.* 2002: p. 267.

51. Suprakas Sinha Ray, and Masami Okamoto, *Biodegradable Polylactide and Its Nanocomposites: Opening a New Dimension for Plastics and Composites, MACROMOLECULAR RAPID COMMUNICATIONS,* 2003(24): p. 815.

52. Carter, L. W; Hendricks, J. G; D.S; 531, 396 *U.S. Patent 2.* 1950.

53. O. Okada, M. Kawasumi, A. Usuki, T. Kuranchi, and O. Kamiagaito, *Mater Res Soc Symp Proc.* 1990(45): p. 171.

54. Jitendra K. Pandey, A. Pratheep Kumar, Manjusri Misra, Amar K. Mohanty, Lawrence T. Drzal, and Raj Pal Singh, *Recent Advances in Biodegradable Nanocomposites. JOURNAL OF NANOSCIENCE AND NANOTECHNOLOGY*, 2005. **5**: p. 497.

55. Michael Mainil, Michael Alexandre, Fabien Monteverde, and Philippe Dubois, *Polyethylene Organo-Clay Nanocomposites: The Role of the Interface Chemistry on the Extent of Clay Intercalation/Exfoliation, JOURNAL OF NANOSCIENCE AND NANOTECHNOLOGY*, 2006. **6**: p. 337.

56. Kazauki Okamato, Suprakash Sinha Ray, and Masami Okamato, *New Poly(butylene succinate)/Layered Silicate Nanocomposites. II. Effect of Organically Modified Layered Silicate on Structure, Properties, Melt Rheology and Biodegradability. JOURNAL OF POLYMER SCIENCE PART B POLYMER PHYSICS*, 2003. **41**: p. 3160.

57. Limin Liu, Zongneng Qi, and Xiaoguang Zhu, *Studies on Nylon 6/Clay Nanocomposites by Melt Intercalation Process. JOURNAL OF APPLIED POLYMER SCIENCE*, 1999. **71**: p. 1133.

58. A. K. Mohanty, M. Misra, and L.T. Drzal, *Polymer Material Science Eng.*, 2003. **88**(61).

59. B. C. Benicewicz, P. K. Hopper, *J. Bioactive Compatible Polym.* 5, 453 (1990) and 6, 64 (1991).

60. D. K. Gilding in: "Biocompatibility of Clinical Omplant Materials", D.F. Williams, Ed., CRC Press, Boca Raton, pp. -232, *BIOCOMPATIBILTY OF CLINICAL OMPLANT MATERIALS.* 1981: p. 209.

61. Stefan Mecking, Angew, *Chem. Int. Ed*, 2004(43): p. 1078.

62. A. K. Mohanty, M. Misra, and L.T. Drzal, Sustainable *Biocomposites From Renewable Resources: Opportunities and Challenges in the Green Material world, JOURNAL OF POLYMERS AND THE ENVIRONMENT*, 2002. **10(1/2)**.

63. Amar K. Mohanty, Manjusri Misra, and Lawrence T. Drzal, *Natural Fibers, Biopolymers, and Biocomposites CRC Taylor and Francis Group*, 2006.

64. Fujimaki, Takashi, *Processing and Properties of Aliphatic Polyesters, 'Bionolle', Synthesized by Polycondensation Reaction. POLYMER DEGRADATION AND STABILITY*, 1998. **59**: p. 209.

65. E. Manias, A. Touny, L. Wu, K. Strawhecker, B. Lu, and T.C. Chung, *Polypropylene/ Montmorillonite Nanocomposites. Review of Synthetic Routes and Material Properties, Chem. Mater.* **13**(2001): p. 3516.

66. Suprakas Sinha Ray and Mosto Bousmina, *Poly(butylene succinate-co-adipate)/Montmorillonite Nanocomposites: Effect of Organic Modifier Miscibility on Structure, Properties and Viscoelasticity. POLYMER*, 2005. **46**: p. 12430.

67. Y. Someya, T. Nakazato, N. Teramoto and M. Shibata, Thermal and Mechanical Properties of poly(butylene succinate) Nanocomposites With Various Organo-Modified Montmorillonites. *JOURNAL OF APPLIED POLYMER SCIENCE*, 2004. **91**: p. 1463.

68. G. Chen, E. Kim and J.S. Yoon, Poly(butylene succinate)/Twice Functionalized Organoclay Nanocomposites: Preparation, Characterization, and Properties, *JOURNAL OF APPLIED POLYMER SCIENCE*, 2005. **98**: p. 1727.

69. Guang-Xin Chen and Jin-San Yoon, *Morphology and Thermal Properties of Poly(L-lactide)/Poly(butylene succinate-co-butylene adipate) Compounded with Twice Functionalized Clay. JOURNAL OF APPLIED POLYMER SCIENCE: PART B: POLYMER PHYSICS*, 2005. **43**: p. 478.

70. Suprakas Sinha Ray, Kazauaki Okamato, Pralay Maiti, and Masami Okamato, *New Poly(butylene succinate)/Layered Silicate Nanocomposites. 1 Preparation and Mechanical Properties. JOURNAL OF NANOSCIENCE AND NANOTECHNOLOGY*, 2002. **2**(2).

71. Doan Thi The, Fumio Yoshii, Naotsugu Nagasawa Tamikazu Kume, *Synthesis of Poly(butylene succinate)/Glass Fiber Composite by Irradiation and Its Biodegradability.JOURNAL OF APPLIED POLYMER SCIENCE*, 2004. **91**: p. 2122.

72. Jo Ann Ratto, P. J. Stenhouse, M. Auerbach, J. Mitchell, and R. Farrell, *Processing, Performance and Biodegradability of a Thermoplastic Aliphatic Polyester/Starch System. POLYMER*, 1999. **40**: p. 6777.

73. Bionolle, Material Safety Data Sheet, Showa Highpolymer Co. Ltd., Japan

74. K. Masenelli-Valo, E. Reynaud, G. Vigier, and J. Varlet, *Mechanical Properties of Clay Reinforced Nanocomposites. JOURNAL OF POLYMER SCIENCE, POLYMER PHYSICS*, 2002. **40**: p. 272

75. Website of Southern Clay Products Inc. Texas accessed 25 July, 2006.

76. Vahik Krikorian and Darrin J. Pochan, *Unusual Crystallization Behavior of Organoclay Reinforced Poly(L-lactic acid) Nanocomposites. MACROMOLECULES*, 2004. **37**: p. 6480.